

# When Measures are Unreliable: Imperceptible Adversarial Perturbations toward Top- $k$ Multi-Label Learning

Yuchen Sun  
IIP, ICT, CAS  
sunyuchen22s@ict.ac.cn

Zitai Wang  
SKLOIS, IIE, CAS  
SCS, UCAS  
wangzitai@iie.ac.cn

Qianqian Xu\*  
IIP, ICT, CAS  
xuqianqian@ict.ac.cn

Qingming Huang\*  
SCST, UCAS  
IIP, ICT, CAS  
BDKM, CAS  
Peng Cheng Laboratory  
qmhuang@ucas.ac.cn

## ABSTRACT

With the great success of deep neural networks, adversarial learning has received widespread attention in various studies, ranging from multi-class learning to multi-label learning. However, existing adversarial attacks toward multi-label learning only pursue the traditional visual imperceptibility but ignore the new perceptible problem coming from measures such as Precision@ $k$  and mAP@ $k$ . Specifically, when a well-trained multi-label classifier performs far below the expectation on some samples, the victim can easily realize that this performance degeneration stems from attack, rather than the model itself. Therefore, an ideal multi-labeling adversarial attack should manage to not only deceive visual perception but also evade monitoring of measures. To this end, this paper first proposes the concept of measure imperceptibility. Then, a novel loss function is devised to generate such adversarial perturbations that could achieve both visual and measure imperceptibility. Furthermore, an efficient algorithm, which enjoys a convex objective, is established to optimize this objective. Finally, extensive experiments on large-scale benchmark datasets, such as PASCAL VOC 2012, MS COCO, and NUS WIDE, demonstrate the superiority of our proposed method in attacking the top- $k$  multi-label systems. Our code is available at: <https://github.com/Yuchen-Sunflower/TKMIA>.

## CCS CONCEPTS

• **Computing methodologies** → **Ranking; Classification and regression trees.**

## KEYWORDS

Top- $k$  Multi-Label Learning, Adversarial Perturbation, Measure Imperceptibility

### ACM Reference Format:

Yuchen Sun, Qianqian Xu, Zitai Wang, and Qingming Huang. 2023. When Measures are Unreliable: Imperceptible Adversarial Perturbations toward Top- $k$  Multi-Label Learning. In *Proceedings of the 31st ACM International*



This work is licensed under a Creative Commons Attribution International 4.0 License.

MM '23, October 29–November 3, 2023, Ottawa, ON, Canada

© 2023 Copyright held by the owner/author(s).

ACM ISBN 979-8-4007-0108-5/23/10.

<https://doi.org/10.1145/3581783.3611846>

Conference on Multimedia (MM '23), October 29–November 3, 2023, Ottawa, ON, Canada. ACM, New York, NY, USA, 22 pages. <https://doi.org/10.1145/3581783.3611846>

## 1 INTRODUCTION

With the rapid development of Deep Neural Networks (DNNs), machine learning has achieved great success in various tasks, such as image recognition [47, 64], text detection [40, 48], and object tracking [33, 49]. However, recent studies have proposed that DNNs are highly vulnerable to the well-crafted perturbations [42, 50, 58]. Due to their intriguing vulnerability, these unguarded models usually suffer from malicious attacks and their performance can be easily affected by slight perturbations hidden behind images. Recently, many pieces of research on adversarial perturbations have found the underlying weakness in practical multimedia applications of DNNs like key text detection [21, 57], video analysis [51, 54], and image super-restoration [8, 61]. The emergence of such problems, which seriously prevent the exploration of various studies and safe applications of DNNs, has raised the attention of many researchers to search for new undetected perturbation technologies, so as to exclude more defense blind spots.

So far, researchers have developed numerous *multi-class* adversarial perturbation algorithms to protect systems. Most of these effective approaches have been widely adopted in real-world classification scenarios [1, 22, 43]. In recent years, more attention has shifted to exploring potential threats in *multi-label* learning [34, 42]. In a multi-label system, common inference strategies can be divided into two categories: *threshold-based* ones and *ranking-based* ones. In the threshold-based approach, the classifier compares the label score with a pre-defined threshold to decide whether each label is relevant to the input sample. Although this strategy is intuitive, the optimal threshold is generally hard to determine. By contrast, the ranking-based approach returns the  $k$  labels with the highest scores as the final prediction, whereas the hyper-parameter  $k$  is much easier to select according to the scenario. Hence, top- $k$  multi-label learning ( $T_k$ ML) has been widely applied to various multimedia-related tasks, such as information retrieval [2, 4] and recommendation systems [7, 27].

\*Corresponding authors.

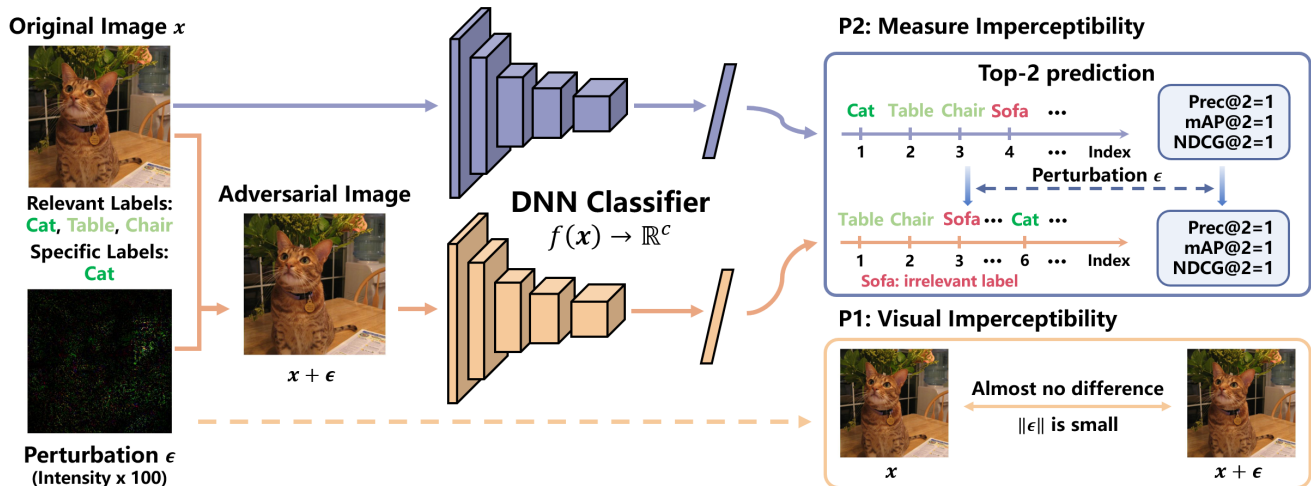


Figure 1: The illustration of the proposed imperceptible adversarial perturbation.

Nevertheless, the majority of current studies on multi-label adversarial perturbations still follow the attack principle on multi-class learning, overly valuing the property of **visual imperceptibility**, but overlooking the new issues that come from the new scenarios. To be specific, for most single-label (multi-class/binary) classifications, when the only relevant category is misclassified, the victim may intuitively attribute the issue to the poor performance of the model, instead of considering whether the attack happens. In contrast, in a multi-label classification scenario, the victim could more likely perceive attacks when all relevant labels are ranked behind the top- $k$  position, as the classification performance of the model is well below the expectation. In view of this, we propose the concept of **measure imperceptibility**. Empirically, we find that it is quite easy to notice the existence of attack by common multi-label measures ranging from Accuracy, Top- $k$  Accuracy ( $T_k$ Acc), to ranking-based measures such as Precision at  $k$  ( $P@k$ ) [31], mean Average Precision at  $k$  (mAP@ $k$ ) [26], and Normalized Discounted Cumulative Gain at  $k$  (NDCG@ $k$ ) [53]. Hence, a natural question arises:

Can we craft a perturbation that satisfies both (P1) visual imperceptibility and (P2) measure imperceptibility?

To answer this question, we introduce a novel algorithm to generate such perturbations for  $T_k$ ML. Specifically, the core challenge lies in constructing an objective function that can disrupt the top- $k$  ranking results in a well-designed manner. To illustrate this, we provide a simple example in Figure 1, where the input image  $x$  has three relevant labels. Our goal is to generate adversarial perturbations that can prevent the classifier from detecting a specified label such as Cat. In order to meet (P1), we need to add a slight perturbation  $\epsilon$  into the image, which makes it almost no different from the original image. To satisfy (P2), we can no longer attack all relevant categories. Instead, the other relevant labels like Table and Chair should be ranked higher to compensate for the performance degeneration induced by the attack on the specified label Cat. Then, the top- $k$  measures, such as  $P@k$ , mAP@ $k$ , and NDCG@ $k$ , will not

drop significantly while the specified label has been ranked far behind the top- $k$  position. In the extreme case, the classifier can never detect certain important categories and produce degraded classification performance, which may result in serious consequences for multimedia applications, such as multimodal emotion recognition [35] and text-to-image generation [20].

Inspired by this example, we construct a novel objective that not only guarantees slight perturbations but also pursues well-designed ranking results. When optimizing this objective, both visual imperceptibility and measure imperceptibility can be achieved. Furthermore, we also propose an effective optimization algorithm to efficiently optimize the perturbation. Finally, we validate the effectiveness of our proposed method on three large-scale benchmark datasets (PASCAL VOC 2012, MS COCO 2014, and NUS WIDE). To summarize, the main contributions of this work are three-fold:

- To the best of our knowledge, we are the pioneer to introduce the vital concept of measure imperceptibility in adversarial multi-label learning.
- We propose a novel imperceptible attack method toward the  $T_k$ ML problem, which enjoys a convex objective. And an efficient algorithm is established to optimize the proposed objective.
- Extensive experiments are conducted on large-scale benchmark datasets including PASCAL VOC 2012, MS COCO 2014, and NUS WIDE. And the empirical results show that the proposed attack method can achieve both visual and measure imperceptibility.

## 2 RELATED WORK

In this section, we will present a brief introduction to multi-class adversarial perturbations, multi-label adversarial perturbations, and top- $k$  ranking optimization.

### 2.1 Multi-class Adversarial Perturbations

**Image-specific Perturbations** is a vital part of adversarial learning, which aims to attack each specific image with a single perturbation. Szegedy *et al.* [45] first observes the vulnerability of DNNs

and gives the corresponding robustness analysis. Then, Goodfellow *et al.* [16] proposes FGSM and describes the important concept of untargeted attack and targeted attack for image-specific perturbations. Inspired by these works, more perturbation methods are gradually emerging to explore these two directions. Specifically, the untargeted attack is an instance-wise attack that increases the scores of irrelevant categories to replace relevant categories in the top- $k$  set. For example, Deepfool [37], as a geometric multi-class untargeted attack, carefully crafts the small perturbation to forge the top-2 class into the correct class. On top of this,  $k$ Fool [46] extends the perturbation to the top- $k$  multi-class learning, designed as the corresponding attacks to replace the ground-truth labels in the top- $k$  set with other irrelevant labels. Different from the above attacks, the targeted attack uses specific negative labels to perturb the predictions. FGSM [16] and I-FGSM [24] conduct back-propagation with the gradient of DNNs to achieve the exploration of minimum efficient perturbation. C&W [5] presents a typical multi-class adversarial learning framework under the top-1 protocol to implement the targeted attack. On the basis of C&W,  $CW^k$  [63] presents an ordered top- $k$  attack by adversarial distillation framework toward top- $k$  multi-class targeted attack. Based on FGSM-based methods, MI-FGSM [12] further introduces the momentum term into an iterative algorithm to avoid coverage into the local optimum.

Our attack method has a similar effect as the untargeted attack, *i.e.*, it replaces the relevant category in the top- $k$  prediction with other several irrelevant labels. The difference is that our perturbation only focuses on specified relevant categories to promise a slight change in measures.

**Image-agnostic Perturbations** is another type of emerging attack based on the untargeted attack, which dedicates to generating an overall perturbation to perturb all points. To the best of our knowledge, Moosavi-Dezfooli *et al.* [36] first introduces Universal Adversarial Perturbations (UAPs) method, which is independent to the single example.  $k$ UAP [46], as the top- $k$  version of UAPs, focuses on top- $k$  universal adversarial learning in multi-class learning. SV-UAP [23] utilizes the singular vectors of the Jacobian matrices of the feature maps to accumulate the minimum perturbation. As interest in UAPs grows recently, a series of related approaches were carried out to further analyze the existing problem in various DNNs-based scenarios [11, 25, 30, 60, 62].

## 2.2 Multi-label Adversarial Perturbations

As far as we know, the first study toward multi-label adversarial attack is [42], in which the authors propose a type of targeted attack, extending image-specific perturbations to multi-label learning. In particular, ML-DP and ML-CW are the multi-label extensions of DeepFool and C&W, respectively. Besides, Melacci *et al.* [34] observe the importance of domain-knowledge constraints for detecting adversarial examples, which analyzes the robustness problem of untargeted attacks in multi-label learning. After realizing the importance of top- $k$  learning in multi-label classification, Hu *et al.* [18] first introduces the image-specific perturbations into top- $k$  multi-label learning, where the untargeted/targeted attack attempts to replace all ground-truth labels in the top- $k$  range with arbitrary/specific  $k$  negative labels. Also, this work is the first to study the vulnerability of  $T_k$ ML.

Despite the great work toward multi-class/label adversarial learning, there is no approach focused on the invisibility of perturbations for measures. By careful consideration, the previous works have been more concerned with the efficiency of the perturbation while ensuring that the perturbation is not visually recognizable. However, the occurrence of these attacks can be easily identified when we pay slight attention to the numerical changes in the measure. In this work, we thus propose an imperceptible adversarial perturbation that could easily deceive the common multi-label metrics to fill this study gap.

## 2.3 Top- $k$ Ranking Optimization

Top- $k$  ranking optimization has a significant amount of applications in various fields, such as binary classification [14, 15], multi-class classification [3, 6, 52], and multi-label learning [19]. Due to the discontinuity of individual top- $k$  error, it is computationally hard to directly minimize the top- $k$  loss. Therefore, the practical solution to the top- $k$ -related problem usually relies on minimizing a differentiable and convex surrogate loss function [59]. In particular, one of the relevant surrogates is the average top- $k$  loss ( $AT_k$ ) [14], which generalizes maximum loss and average loss to better fit the optimization in different data distributions, especially for imbalanced problems. On top of this work, Hu *et al.* further propose a summation version of the top- $k$  loss called "Sum of Ranked Range (SoRR)", and demonstrate its effectiveness in top- $k$  multi-label learning [19]. Both of these surrogates are convex with respect to each individual loss, which means optimizing the objective function only needs simple gradient-based methods.

Inspired by these discoveries, we introduce the  $AT_k$  into our algorithm to further improve the performance of our method. More details about the technology we used to optimize perturbations could be found in Sec.3.2.

## 3 PRELIMINARIES

In this section, we first give the used notation in the following content and introduce the average of top- $k$  optimization method.

### 3.1 Notations

Generally, we assume that the samples are drawn *i.i.d* from the space  $\mathcal{Z} = \mathcal{X} \times \mathcal{Y}$ , where  $\mathcal{X}$  is the input space;  $\mathcal{Y} = \{0, 1\}^c$  is the label space with 1 for positive and 0 for negative;  $c$  represents the number of labels. In multi-label learning, each input  $\mathbf{x} \in \mathcal{X}$  is associated with a label vector  $\mathbf{y} \in \mathcal{Y}$ . We use  $Y_p = \{i | y_i = 1\}$  and  $Y_n = \{j | y_j = 0\}$  to denote the relevant labels and irrelevant labels of  $\mathbf{x}$ , respectively, where  $y_i$  is the  $i$ -th element of  $\mathbf{y}$ .

Then, our task is to learn a multi-label prediction function  $F(\mathbf{x}) = [f_1(\mathbf{x}), \dots, f_c(\mathbf{x})] : \mathcal{X} \rightarrow \mathbb{R}^c$  to estimate the relevancy score for each class. For each component of  $F$ ,  $f_i(\mathbf{x}) \in [0, 1]$  denotes the prediction score of  $i$ -th class. In ranking values, we define  $f_{[i]}(\mathbf{x})$  as the  $i$ -th largest element of  $F(\mathbf{x})$ , that is,  $f_{[1]}(\mathbf{x}) \geq f_{[2]}(\mathbf{x}) \geq \dots \geq f_{[c]}(\mathbf{x})$ . In the following content, we uniformly assume that the ties between any two prediction scores are completely broken, *i.e.*,  $f_{[1]}(\mathbf{x}) > \dots > f_{[c]}(\mathbf{x})$ .

### 3.2 Average of Top- $k$ Optimization

Top- $k$  optimization, which is a useful tool to construct our objective, has been widely applied to various tasks like information retrieval [29] and recommendation systems [32]. For  $T_k$ ML, it is intuitive to construct an objective function such that the lowest value of the predicted score for the relevant category is higher than the  $(k + 1)$ -th largest score [19]:

$$\min_{y \in Y_p} f_y(\mathbf{x}) > f_{[k+1]}(\mathbf{x}).$$

And this idea has been successfully applied to generate top- $k$  multi-label adversarial perturbation [18], making the perturbed image satisfy that:

$$\max_{y \in Y_p} f_y(\mathbf{x} + \epsilon) < f_{[k+1]}(\mathbf{x} + \epsilon).$$

In other words, this objective expects the highest score of the relevant labels is not ranked before the top- $k$  position. However, due to the non-differentiable ranking operator, the individual top- $k$  loss is not easy to optimize [14, 59]. To address this issue, a series of surrogate loss functions including the sum of ranked range [19], average top- $k$  loss [14], are proposed. To be specific, for a set of  $F(\mathbf{x})$ , the average top- $k$  loss  $\phi_k(F(\mathbf{x}))$  is defined as

$$\phi_k(F(\mathbf{x})) = \frac{1}{k} \sum_{i=1}^k f_{[i]}(\mathbf{x}), \quad (1)$$

which is proven convex *w.r.t* each component. For this expression, we could directly see that  $\phi_k(F(\mathbf{x}))$  is the upper bound of  $f_{[k]}(\mathbf{x})$ , *i.e.*,  $\phi_k(F(\mathbf{x})) \geq f_{[k]}(\mathbf{x})$ . Hence, this fact provides a convex equivalent form for the original top- $k$  optimization problem.

## 4 MEASURE IMPERCEPTIBLE ATTACK

In this section, we define the concept of measure-imperceptible attack and further present the corresponding imperceptible attack algorithm.

### 4.1 Problem Formation

This measure-imperceptible attack attempts to attack a few categories while not degenerating the performance of ranking measures. To achieve this goal, we need to

- **G1**: rank the specific relevant categories lower than the  $k$ -th position;
- **G2**: rank the other relevant categories higher than the  $k$ -th position as much as possible;
- **G3**: generate an visual imperceptible perturbation  $\epsilon$  that is as smaller as possible.

According to these sub-goals, we could utilize the existing symbols to form the following optimization problem:

$$\begin{aligned} \min_{\epsilon} \|\epsilon\|_2 + \underbrace{f_{[k]}(\mathbf{x} + \epsilon) - \min_{y \in Y_p \setminus \mathcal{S}} f_y(\mathbf{x} + \epsilon)}_{c_2} \\ \text{s.t. } \underbrace{f_{[k+1]}(\mathbf{x} + \epsilon) \geq \max_{s \in \mathcal{S}} f_s(\mathbf{x} + \epsilon)}_{c_1}, \end{aligned} \quad (2)$$

where  $\mathcal{S}$  is the specified label set that includes partial indices of the relevant categories of a sample  $\mathbf{x}$ .

Specifically, the condition  $c_1$  guarantees that all specified categories cannot be ranked higher than the top- $k$  position,  $c_2$  requires the top- $k$  set to be filled with a certain amount of other relevant labels, and the regularizer limits the size of perturbations, respectively. These three constraints correspond to the above three sub-goals. However, it is challenging to optimize due to the complex constraints of this problem. Consequently, we expect to seek a more easily optimized formulation to solve this problem.

### 4.2 Optimization Relaxation

To optimize the problem in Eq.(2), it is necessary to build a feasible optimization framework. To begin with, we could notice that for a well-trained model, most of the specified categories of an image are possibly ranked higher than the  $k$ -th largest score, that is,

$$\max_{s \in \mathcal{S}} f_s(\mathbf{x} + \epsilon) - f_{[k+1]}(\mathbf{x} + \epsilon) \geq 0.$$

Meanwhile, there exist a few ground-truth labels that are not in the top- $k$  set, and they satisfy the condition that:

$$f_{[k]}(\mathbf{x} + \epsilon) - \min_{y \in Y_p \setminus \mathcal{S}} f_y(\mathbf{x} + \epsilon) \geq 0.$$

Thus, the original problem (2) could be transformed to reduce the loss generated by combining the above two equations and the perturbation norm. Utilizing the Lagrangian equation, we obtain this surrogate loss function:

$$\begin{aligned} \min_{\epsilon} \frac{\alpha}{2} \|\epsilon\|_2^2 + \left[ \max_{s \in \mathcal{S}} f_s(\mathbf{x} + \epsilon) - f_{[k+1]}(\mathbf{x} + \epsilon) \right]_+ \\ + \left[ f_{[k]}(\mathbf{x} + \epsilon) - \min_{y \in Y_p \setminus \mathcal{S}} f_y(\mathbf{x} + \epsilon) \right]_+, \end{aligned} \quad (3)$$

where  $\alpha$  is the trade-off hyper-parameter. However, the potential gradient sparsity problem [59] of Eq.(3) makes the optimization very hard. To solve this problem, we could further leverage Eq.(1) to form an equivalent convex relaxation. And the following lemma also provides us with a solution for the average top- $k$  optimization:

**LEMMA 4.1** ([38]). *For  $\lambda \in [0, 1]$ ,  $f_i(\mathbf{x}) \in [0, 1]$ ,  $i = 1, \dots, c$ , we have*

$$\sum_{i=1}^k f_{[i]}(\mathbf{x}) = \min_{\lambda \in [0, 1]} \{k\lambda + \sum_{i=1}^c [f_i(\mathbf{x}) - \lambda]_+\},$$

where  $[a]_+ = \max\{0, a\}$ , and  $f_{[k]}(\mathbf{x})$  is one optimal solution.

Thus by adopting Lem.4.1 to Eq.(1), a convex optimization framework could be established. We will show this specific relaxation process of our objective below.

**Relaxation of  $c_1$ .** For the sake of explanation, we first make the definitions of  $\Delta_i$  and  $\Delta_{[i]}$ , which measure the difference between the maximum score of all specified labels and the  $i$ -th/bottom- $i$  score of all labels, respectively, *i.e.*,

$$\begin{aligned} \Delta_i &= \left[ \max_{s \in \mathcal{S}} f_s(\mathbf{x} + \epsilon) - f_i(\mathbf{x} + \epsilon) \right]_+, \\ \Delta_{[i]} &= \left[ \max_{s \in \mathcal{S}} f_s(\mathbf{x} + \epsilon) - f_{[c-i+1]}(\mathbf{x} + \epsilon) \right]_+. \end{aligned} \quad (4)$$

When  $i = 1$ ,  $\Delta_{[1]}$  is the largest difference since  $f_{[c]}(\mathbf{x} + \epsilon)$  is the smallest value among  $c$  scores. It could be known that as  $i$  increases, the value of  $f_{[c-i+1]}(\mathbf{x} + \epsilon)$  increases consistently and the difference



$\Delta_{[i]}$  reduces. Thus,  $\Delta_{[i]}$  refers to the  $i$ -th largest element among  $\Delta_i$ . Then, according to the fact

$$\frac{1}{c-k} \sum_{i=1}^{c-k} \Delta_{[i]} \geq \Delta_{[c-k]},$$

and Lem.4.1, we have

$$\min_{\lambda_1 \in [0,1]} \lambda_1 + \frac{1}{c-k} \sum_{i=1}^c [\Delta_i - \lambda_1]_+.$$

Furthermore, we could remove the inner redundant hinge function by the following lemma:

**LEMMA 4.2** ([14]). *For  $\forall a > 0, b > 0$ , we have  $[[a-x]_+ - b]_+ = [a-x-b]_+$ .*

Then, the second term in Eq.(3) could be finally transformed into

$$\min_{\lambda_1 \in [0,1]} \lambda_1 + \frac{1}{c-k} \sum_{i=1}^c \left[ \max_{s \in \mathcal{S}} f_s(\mathbf{x} + \epsilon) - f_i(\mathbf{x} + \epsilon) - \lambda_1 \right]_+.$$

**Relaxation of  $c_2$ .** Similarly, we could make the definitions of  $\tilde{\Delta}_j$  and  $\tilde{\Delta}_{[j]}$  to convert the third term of Eq.(3):

$$\begin{aligned} \tilde{\Delta}_j &= \left[ f_j(\mathbf{x} + \epsilon) - \min_{y \in Y_p \setminus \mathcal{S}} f_y(\mathbf{x} + \epsilon) \right]_+, \\ \tilde{\Delta}_{[j]} &= \left[ f_{[j]}(\mathbf{x} + \epsilon) - \min_{y \in Y_p \setminus \mathcal{S}} f_y(\mathbf{x} + \epsilon) \right]_+, \end{aligned} \quad (5)$$

where  $\tilde{\Delta}_{[j]}$  is the  $j$ -th largest element among  $\tilde{\Delta}_j$ . Correspondingly, its final optimization could be written as:

$$\min_{\lambda_2 \in [0,1]} \lambda_2 + \frac{1}{k} \sum_{j=1}^c \left[ f_j(\mathbf{x} + \epsilon) - \min_{y \in Y_p \setminus \mathcal{S}} f_y(\mathbf{x} + \epsilon) - \lambda_2 \right]_+.$$

Combining the above two objectives, we obtain our final objective. The final objective is shown as follows:

$$\begin{aligned} \min_{\lambda_1, \lambda_2 \in [0,1], \epsilon} & \lambda_1 + \lambda_2 + \frac{\alpha}{2} \|\epsilon\|_2^2 \\ & + \frac{1}{c-k} \sum_{i=1}^c \left[ \max_{s \in \mathcal{S}} f_s(\mathbf{x} + \epsilon) - f_i(\mathbf{x} + \epsilon) - \lambda_1 \right]_+ \\ & + \frac{1}{k} \sum_{j=1}^c \left[ f_j(\mathbf{x} + \epsilon) - \min_{y \in Y_p \setminus \mathcal{S}} f_y(\mathbf{x} + \epsilon) - \lambda_2 \right]_+. \end{aligned} \quad (6)$$

In this way, our original single-element optimization problem is modified into a form of average top- $k$  optimization. This objective does not depend on any sorted result but just needs to calculate the sum result, which greatly reduces the complexity of optimizing perturbations. To solve this optimization problem, we could utilize the iterative gradient descent method [18, 19] to directly update  $\epsilon$  and  $\lambda_i$  with the following **Algorithm 1**. For this algorithm, we would adopt two different selection schemes to select specified categories:

- **S1: Global Selection.** In this case, we globally specify several categories for all the samples. Note that only the samples relevant to at least one specific category are attacked.

- **S2: Random Selection.** In this case, we randomly specify  $m$  ground-truth labels for each example. For any integer  $m$ , it satisfies that  $0 < m \leq k$ .

---

**Algorithm 1:** Top- $k$  Measure Imperceptible Attack (T<sub>k</sub>MIA)

---

**Input:** example  $\mathbf{x}$ , predictor  $F$ , learning rate  $\eta$ , maximum iteration  $L$ , specified label set  $\mathcal{S}$

**Output:** Optimal perturbation  $\epsilon^{l+1}$ , adversarial example  $\mathbf{x}^*$

1 **Initialization:**  $\epsilon^0 = 0, \mathbf{x}^* = \mathbf{x}, l = 0$

2 **while**  $l < L$  **do**

3     Calculate the gradients of Eq.(6):  $\nabla \lambda_1^l, \nabla \lambda_2^l$  and  $\nabla \epsilon^l$

4      $\lambda_1^{l+1} = \lambda_1^l - \eta \nabla \lambda_1^l, \lambda_2^{l+1} = \lambda_2^l - \eta \nabla \lambda_2^l$

5     Update  $\mathbf{x}^* = \mathbf{x}^* + \epsilon^{l+1}$  where  $\epsilon^{l+1} = \epsilon^l - \eta \nabla \epsilon^l$

6     **if** conditions of Eq.(2) hold **then**

7         **break**

8     **end**

9 **end**

10 **return**  $\mathbf{x}^*, \epsilon^{l+1}$

---

## 5 EXPERIMENTS

In this section, we present the experimental settings and evaluate the quantitative results of our method against other comparison methods on three large-scale benchmark datasets and two attack schemes.

### 5.1 Experimental Settings

**Datasets.** We carry out our experiments on three well-known benchmark multi-label image annotation datasets containing PASCAL VOC 2012 (VOC) [13], MS COCO 2014 (COCO) [28] and NUS WIDE (NUS) [9]. Considering space constraints, we present the information about these datasets in Appendix B.1

**Evaluation Metrics.** For each individual experiment, we would report Multi-label Top- $k$  accuracy (T<sub>k</sub>Acc) and three popular ranking-based measures for a more comprehensive comparison, including Precision at  $k$  (P@ $k$ ), mean Average Precision at  $k$  (mAP@ $k$ ) and Normalized Discounted Cumulative Gain at  $k$  (NDCG@ $k$ ).

With a bit of abuse of the notation, we use  $\pi$  to denote the indices of permutations of  $F(\mathbf{x})$ . For the instance  $z = (\mathbf{x}, \mathbf{y})$  and model  $F$ ,  $\pi_k(F, z) = \{[1], \dots, [k]\}$  denotes the top- $k$  classes *w.r.t* input  $\mathbf{x}$ . Hence, the Multi-label Top- $k$  Accuracy [19] is defined as follows:

$$\text{T}_k \text{Acc}(F, z) = \mathbb{I}_{[Y_p \subseteq \pi_k(F, z)]}, \quad (7)$$

where  $\mathbb{I}_{[\cdot]}$  is the indicator function. Then, we make the following definition of Precision at  $k$  [31]:

$$\text{P}@k(f, \mathbf{y}) = \frac{1}{k} \sum_{i=1}^k y_{[i]}. \quad (8)$$

As an extended concept, Average Precision at  $k$  [41, 56] averages the top- $k$  precision performance at different recall values:

$$\text{AP}@k(f, \mathbf{y}) = \frac{1}{N_k(\mathbf{y})} \sum_{i=1}^k y_{[i]} \cdot \text{P}@k, \quad (9)$$

**Table 1: The average performance with the maximum iteration 300 under different  $k$  values and globally selected  $S$  on COCO, where  $\Delta$  refers to the difference between the original value and the perturbed value of corresponding metrics.  $\downarrow$  means the smaller the value the better, and  $\uparrow$  is the opposite. The best results under each set of parameters are bolded.**

Type	$k$	Methods	$\Delta T_k \text{Acc} \downarrow$	$\Delta P@k \downarrow$	$\Delta mAP@k \downarrow$	$\Delta NDCG@k \downarrow$	$\Delta l \uparrow$	APer $\downarrow$
Person	3	ML-CW-U	0.6400	0.4607	0.6064	0.5409	0.9960	1.9235
		kFool	0.4820	0.2643	0.2909	0.2297	0.6540	3.0603
		$T_k$ ML-AP-U	0.6290	0.4466	0.5860	0.5213	1.0000	1.5846
		$T_k$ MIA(Ours)	<b>0.1880</b>	<b>0.1073</b>	<b>0.1320</b>	<b>0.1081</b>	<b>1.0000</b>	<b>1.2314</b>
	5	ML-CW-U	0.3840	0.5288	0.6872	0.6459	0.9930	2.4513
		kFool	0.2920	0.2514	0.2989	0.2405	0.6570	12.5931
		$T_k$ ML-AP-U	0.3710	0.4904	0.6573	0.6105	0.9980	2.0422
		$T_k$ MIA(Ours)	<b>0.0670</b>	<b>0.0844</b>	<b>0.1161</b>	<b>0.0909</b>	<b>1.0000</b>	<b>1.6404</b>
	10	ML-CW-U	0.1098	0.5366	0.7097	0.6716	0.9756	2.7744
		kFool	0.0732	0.1927	0.2501	0.1934	0.5976	4.8946
		$T_k$ ML-AP-U	0.1097	0.4646	0.6699	0.6137	0.9878	2.3951
		$T_k$ MIA(Ours)	<b>0.0000</b>	<b>0.0707</b>	<b>0.0933</b>	<b>0.0627</b>	<b>1.0000</b>	<b>1.4923</b>

**Table 2: The average performance with the maximum iteration 300 under globally selected  $S$  on NUS.**

Type	$k$	Methods	$\Delta T_k \text{Acc} \downarrow$	$\Delta P@k \downarrow$	$\Delta mAP@k \downarrow$	$\Delta NDCG@k \downarrow$	$\Delta l \uparrow$	APer $\downarrow$
Buildings	2	ML-CW-U	0.4410	0.2725	0.3215	0.2787	0.9820	1.2455
		kFool	0.5350	0.4210	0.4455	0.4174	1.0030	14.2177
		$T_k$ ML-AP-U	0.4290	0.2650	0.3162	0.2742	0.9710	1.0741
		$T_k$ MIA(Ours)	<b>0.2500</b>	<b>0.1630</b>	<b>0.1745</b>	<b>0.1537</b>	<b>1.0040</b>	<b>0.7156</b>
	3	ML-CW-U	0.5060	0.2703	0.3482	0.2896	0.9440	1.6943
		kFool	0.6300	0.4890	0.5315	0.4829	<b>1.0160</b>	23.6683
		$T_k$ ML-AP-U	0.5200	0.2870	0.3720	0.3116	0.9480	1.5096
		$T_k$ MIA(Ours)	<b>0.2830</b>	<b>0.1373</b>	<b>0.1483</b>	<b>0.1172</b>	1.0120	<b>0.8673</b>
	5	ML-CW-U	0.3383	0.2419	0.3391	0.2859	0.7626	2.1203
		kFool	0.4131	0.4441	0.5027	0.4414	<b>1.0579</b>	38.9787
		$T_k$ ML-AP-U	0.3530	0.2665	0.3840	0.3283	0.7943	1.9588
		$T_k$ MIA(Ours)	<b>0.2224</b>	<b>0.1237</b>	<b>0.1315</b>	<b>0.0975</b>	1.0318	<b>1.2240</b>

where  $N_k(\mathbf{y}) = \min\{k, |Y_p|\}$ , and mean Average Precision at  $k$  [26, 55] measures AP performance on each category:

$$mAP@k(f, \mathbf{y}) = \frac{1}{c} \sum_{j=1}^c AP_j@k(f, \mathbf{y}), \quad (10)$$

where  $AP_j@k(f, \mathbf{y})$  refers to the AP performance on  $j$ -th category.

Normalized Discounted Cumulative Gain at  $k$  (NDCG@ $k$ ) [53] is a kind of listwise ranking measure that allocates decreasing weights to the labels from top to bottom positions, so as to precisely evaluate each ranking result:

$$\begin{aligned} DCG@k(f, \mathbf{y}) &= \sum_{i=1}^k \frac{y_{[i]}}{\log_2(i+1)}, \\ IDC@k(\mathbf{y}) &= \sum_{i=1}^{N_k(\mathbf{y})} \frac{1}{\log_2(i+1)}, \\ NDCG@k(f, \mathbf{y}) &= \frac{DCG@k(f, \mathbf{y})}{IDCG@k(\mathbf{y})}. \end{aligned} \quad (11)$$

To further measure the overall effectiveness of our perturbation algorithm, it is necessary to evaluate the success rate and size of the perturbation. We now define the average attack effectiveness

metric  $\Delta l$ , which calculates the average change number of top- $k$  specified relevant labels over all images:

$$\Delta l = \frac{1}{n} \sum_{i=1}^n (|S| - |S'|), \quad (12)$$

where  $S'$  is the labels in  $S$  that are still ranked in the top- $k$  region after attacking. And average perturbation (APer), which measures the average successful perturbation among all instances, is presented as:

$$APer = \frac{1}{n} \sum_{i=1}^n \|\epsilon_i\|_2. \quad (13)$$

**Competitors.** We compare our method with the existing top- $k$  multi-label untargeted attack methods, encompassing  $T_k$ ML-AP-U [18],  $k$ Fool [46] and ML-CW-U [5], since their process of excluding the top- $k$  relevant labels is similar to ours. However, all of them are untargeted attacks and not for the specified categories. For the sake of fairness, we uniformly ask these methods to attack specified categories in the top- $k$  set. Then, we observe the norm of successful perturbation and its metric change. Due to length limitations, we have relegated their details to Appendix B.2.

**Table 3: The average performance with the maximum iteration 300 and  $\delta = 2$  under randomly selected  $S$  on COCO.**

$k$	$ S $	Methods	$\Delta T_k \text{Acc} \downarrow$	$\Delta P@k \downarrow$	$\Delta mAP@k \downarrow$	$\Delta NDCG@k \downarrow$	$\Delta I \uparrow$	APer $\downarrow$
5	2	ML-CW-U	0.4900	0.5232	0.6767	0.6177	1.9970	2.0903
		$k$ Fool	0.4640	0.3846	0.4694	0.3898	1.6000	59.2396
		$T_k$ ML-AP-U	0.4890	0.5042	0.6638	0.6026	2.0000	1.7409
		$T_k$ MIA(Ours)	<b>0.3680</b>	<b>0.2236</b>	<b>0.2641</b>	<b>0.2207</b>	<b>2.0000</b>	<b>1.0922</b>
	3	ML-CW-U	0.5780	0.3416	0.5057	0.4158	2.0100	1.9175
		$k$ Fool	0.5060	0.2636	0.3320	0.2499	1.8510	30.6267
		$T_k$ ML-AP-U	0.5740	0.3274	0.5018	0.4117	2.0260	1.5879
		$T_k$ MIA(Ours)	<b>0.5020</b>	<b>0.2130</b>	<b>0.2731</b>	<b>0.2091</b>	<b>2.0590</b>	<b>1.2568</b>
	5	ML-CW-U	0.6505	0.1689	0.2294	0.1605	2.0097	1.5667
		$k$ Fool	0.5097	0.1281	0.1539	0.0988	<b>2.0291</b>	5.7119
		$T_k$ ML-AP-U	0.6116	0.1543	0.2127	0.1476	2.0097	1.3096
		$T_k$ MIA(Ours)	<b>0.4563</b>	<b>0.1146</b>	<b>0.1413</b>	<b>0.0940</b>	2.0049	<b>1.0605</b>

**Table 4: The average performance with the maximum iteration 300 and  $\delta = 2$  under randomly selected  $S$  on NUS.**

$k$	$ S $	Methods	$\Delta T_k \text{Acc} \downarrow$	$\Delta P@k \downarrow$	$\Delta mAP@k \downarrow$	$\Delta NDCG@k \downarrow$	$\Delta I \uparrow$	APer $\downarrow$
5	2	ML-CW-U	0.5240	0.3970	0.5204	0.4519	1.3400	2.6046
		$k$ Fool	0.5980	0.5912	0.6585	0.6010	<b>1.8900</b>	121.4293
		$T_k$ ML-AP-U	0.5500	0.4854	0.6164	0.5527	1.6300	2.2604
		$T_k$ MIA(Ours)	<b>0.3990</b>	<b>0.2334</b>	<b>0.2653</b>	<b>0.2001</b>	1.6070	<b>1.9674</b>
	3	ML-CW-U	0.5564	0.2877	0.3856	0.3087	1.5063	2.4936
		$k$ Fool	0.6118	0.3445	0.4190	0.3283	<b>2.0178</b>	38.8708
		$T_k$ ML-AP-U	0.5831	0.3359	0.4682	0.3843	1.7280	<b>2.1731</b>
		$T_k$ MIA(Ours)	<b>0.4615</b>	<b>0.2228</b>	<b>0.2594</b>	<b>0.1888</b>	1.7602	2.1984
	5	ML-CW-U	0.5833	0.1583	0.2096	0.1413	1.7083	1.9930
		$k$ Fool	<b>0.5416</b>	0.1416	0.1700	0.1138	<b>2.2083</b>	3.1938
		$T_k$ ML-AP-U	0.5833	0.1583	0.1979	0.1361	1.7916	<b>1.5910</b>
		$T_k$ MIA(Ours)	0.5833	<b>0.1416</b>	<b>0.1541</b>	<b>0.0998</b>	1.9583	1.6672

Since these competitors hardly achieve measure imperceptibility, it is unfair to require all of them to meet the strict constraints in Eq.(2). Thus, we uniformly lower the judging standard of a successful perturbation. Note that when the number of excluded specified categories is no less than threshold  $\delta$  after a certain iteration, we term it a successful attack. We set  $\delta = |S|$  for **S1**, and ask this integer no larger than  $|S|$  for **S2**, respectively. In this case, we compare each baseline with our method by observing the value change of measures and average perturbation norm.

**Implementation Details.** Our experiments are implemented by PyTorch [39], running on NVIDIA TITAN RTX with CUDA v12.0. We select ResNet-50 [17] as the backbone on VOC, and ResNet-101 [17] on COCO and NUS, respectively. All parameters are initialized with the checkpoint pre-trained on ImageNet, except for the randomly initialized fully connected layer. To satisfy the multi-label classification tasks, we add the sigmoid function to keep the output results ranging from  $[0, 1]$ . All pixel intensities of each RGB image range from  $\{0, 1, \dots, 255\}$ . More details about the models we used on each dataset are presented in Appendix B.3.

At the attack period, all images are normalized into the range of  $[-1, 1]$ . We adopt SGD [44] as our optimizer, where both learning rate and hyper-parameter  $\alpha$  are searched within the range of  $\{1e-3, 5e-4, 1e-4, 5e-5\}$ , and momentum adopts 0.9. All of the victim models are well-trained so as to promise the effectiveness of our attack

under various specified categories. On top of this, we only sample the instance that satisfies  $|Y_p| \geq k + |S|$  from the validation set as the attack objects. The maximum number of test images under each set of parameters is set as 1000, and the maximum iteration ranges from  $\{100, 300, 500\}$ .

## 5.2 Results Analysis

The average performance of  $T_k$ MIA (1) under the global selection scheme (2) on COCO and NUS are shown in Table 1 and Table 2, respectively, where the categories included in each type are specifically illustrated in Appendix B.4. In most cases,  $T_k$ MIA outperforms other comparison methods when  $k$  and  $|S|$  take different values. It could achieve a smaller change in each metric while perturbing more specified categories in  $S$ . Although  $k$ Fool attacks more classes in some cases, it comes at a larger cost to generate the perturbation. Furthermore, Figure 2 clearly shows the visual effect of our attack method and other comparison methods in the global selection scheme on NUS. All competitors could manage to remove the specified class from the top- $k$  prediction. However, they raise the scores of several irrelevant categories, making them appear in the top- $k$  predictions, resulting in the performance degradation of measures. Our perturbation considers increasing the scores of other relevant categories in addition to perturbing these specified labels to achieve the effect of confusing the metrics. On the other

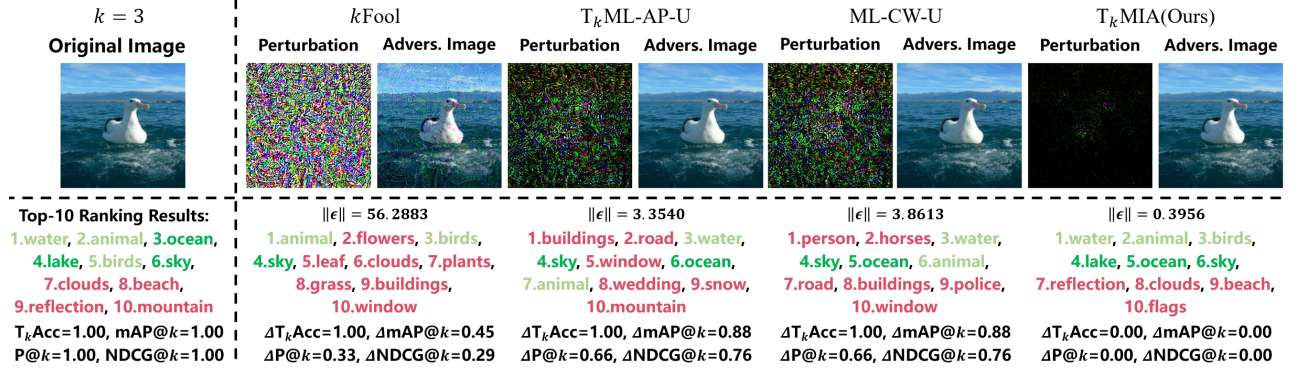


Figure 2: The top-3 successful performance comparisons under *global selection scheme* on NUS, where the maximum iteration is 300. All perturbation intensities are magnified by a factor of 100 to enhance contrast and visibility. The specified labels, relevant labels, and irrelevant labels are marked with **dark green**, **light green**, and **red**, respectively.

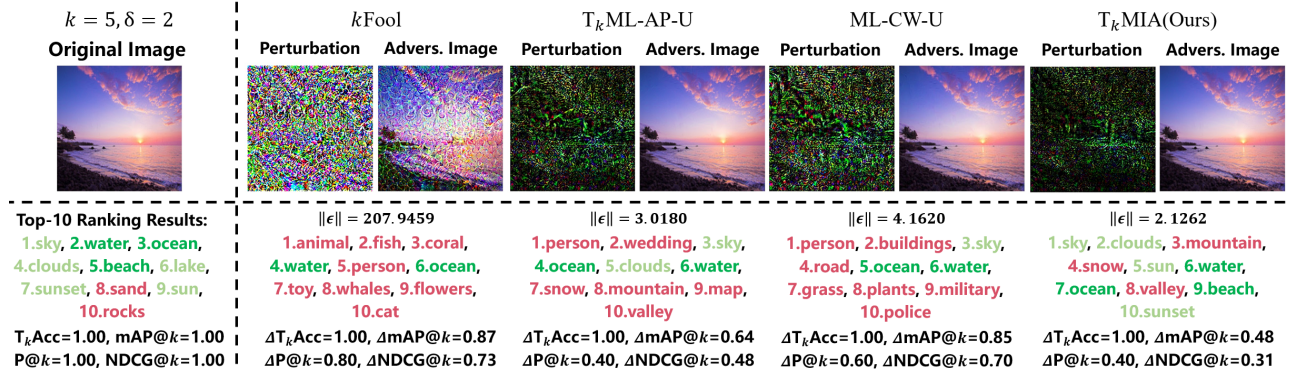


Figure 3: The top-5 successful performance comparisons under *random selection scheme* on NUS, where the maximum iteration is 300. All perturbation intensities are magnified by a factor of 100 to enhance contrast and visibility. The specified labels, relevant labels, and irrelevant labels are marked with **dark green**, **light green**, and **red**, respectively.

hand, our method achieves this goal with a smaller perturbation which could hardly be discerned. These results and analysis all demonstrate that  $T_k$ MIA could achieve both visual and measure imperceptibility in the global selection scheme.

Table 3 and Table 4 present the comparative average performance of different methods under different parameters (1) in the random selection scheme (2) on COCO and NUS, respectively. For the measure performance, our perturbation performs better than other baselines. However, an interesting phenomenon is that  $k$ Fool perturbs more labels while paying a huge effort, and  $T_k$ ML-AP-U generates a relatively smaller perturbation but only obtains the sub-optimal metric change results. The proposed  $T_k$ MIA makes a trade-off between visual imperceptibility and measure imperceptibility and achieves a better overall performance on  $\Delta I$  and APer. The visualization results of an example under the random selection scheme on NUS are shown in Figure 3. Comparing these value changes in metrics, we can see that  $T_k$ MIA always promises a smaller change so as to make its perturbation not obvious. Even if there are still some irrelevant labels in the top- $k$  set, our method also tries to prevent them from being in the front position. This means the proposed perturbation is more favorable to maintaining the measure imperceptibility. Other experimental results and analyses on VOC, COCO, and NUS are presented in Appendix C.

## 6 CONCLUSION

In this paper, we propose a method named  $T_k$ MIA to generate a novel adversarial perturbation toward top- $k$  multi-label classification models, which could satisfy both visual imperceptibility and measure imperceptibility to better evade the monitoring of defenders. To achieve this goal, we form a simple and convex objective with a corresponding gradient iterative algorithm to effectively optimize this perturbation. Finally, a series of empirical studies on different large-scale benchmark datasets and schemes are carried out. Extensive experimental results and analysis validate the effectiveness of the proposed method.

## ACKNOWLEDGMENTS

This work was supported in part by the National Key R&D Program of China under Grant 2018AAA0102000, in part by National Natural Science Foundation of China: 62236008, U21B2038, 61931008, 6212200758 and 61976202, in part by the Fundamental Research Funds for the Central Universities, in part by Youth Innovation Promotion Association CAS, in part by the Strategic Priority Research Program of Chinese Academy of Sciences, Grant No. XDB28000000.

## REFERENCES

- [1] Sandhya Aneja, Nagender Aneja, Pg Emeroylariffion Abas, and Abdul Ghani Naim. 2022. Defense against adversarial attacks on deep convolutional neural networks through nonlocal denoising. *CoRR abs/2206.12685* (2022).
- [2] Carlos Bermejo, Tristan Braud, Ji Yang, Shayan Mirjafari, Bowen Shi, Yu Xiao, and Pan Hui. 2020. VIMES: A Wearable Memory Assistance System for Automatic Information Retrieval. In *ACM International Conference on Multimedia*. 3191–3200.
- [3] Leonard Berrada, Andrew Zisserman, and M. Pawan Kumar. 2018. Smooth Loss Functions for Deep Top- $k$  Classification. In *International Conference on Learning Representations*.
- [4] Maurits J. R. Bleeker. 2022. Multi-modal Learning Algorithms and Network Architectures for Information Extraction and Retrieval. In *ACM International Conference on Multimedia*. 6925–6929.
- [5] Nicholas Carlini and David A. Wagner. 2017. Towards Evaluating the Robustness of Neural Networks. In *IEEE Symposium on Security and Privacy*. 39–57.
- [6] Xiaojun Chang, Yaoliang Yu, and Yi Yang. 2017. Robust Top- $k$  Multiclass SVM for Visual Category Recognition. In *ACM SIGKDD International Conference on Knowledge Discovery and Data Mining*. 75–83.
- [7] Junyu Chen, Qianqian Xu, Zhiyong Yang, Ke Ma, Xiaochun Cao, and Qingming Huang. 2022. Recurrent Meta-Learning against Generalized Cold-start Problem in CTR Prediction. In *ACM International Conference on Multimedia*. 2636–2644.
- [8] Jun-Ho Choi, Huan Zhang, Jun-Hyuk Kim, Cho-Jui Hsieh, and Jong-Seok Lee. 2019. Evaluating Robustness of Deep Image Super-Resolution Against Adversarial Attacks. In *IEEE/CVF International Conference on Computer Vision*. 303–311.
- [9] Tat-Seng Chua, Jinhui Tang, Richang Hong, Haojie Li, Zhiping Luo, and Yantao Zheng. 2009. NUS-WIDE: a real-world web image database from National University of Singapore. In *ACM International Conference on Image and Video Retrieval*.
- [10] Jia Deng, Wei Dong, Richard Socher, Li-Jia Li, Kai Li, and Li Fei-Fei. 2009. ImageNet: A large-scale hierarchical image database. In *IEEE Conference on Computer Vision and Pattern Recognition*. 248–255.
- [11] Yingpeng Deng and Lina J. Karam. 2022. Frequency-Tuned Universal Adversarial Attacks on Texture Recognition. *IEEE Trans. Image Process.* 31 (2022), 5856–5868.
- [12] Yinpeng Dong, Fangzhou Liao, Tianyu Pang, Hang Su, Jun Zhu, XiaoLin Hu, and Jianguo Li. 2018. Boosting Adversarial Attacks With Momentum. In *IEEE Conference on Computer Vision and Pattern Recognition*. 9185–9193.
- [13] Mark Everingham, S. M. Ali Eslami, Luc Van Gool, Christopher K. I. Williams, John M. Winn, and Andrew Zisserman. 2015. The Pascal Visual Object Classes Challenge: A Retrospective. *International Journal of Computer Vision* (2015), 98–136.
- [14] Yanbo Fan, Siwei Lyu, Yiming Ying, and Bao-Gang Hu. 2017. Learning with Average Top- $k$  Loss. In *Annual Conference on Neural Information Processing Systems*. 497–505.
- [15] Jordan Fréry, Amaury Habrard, Marc Sebban, Olivier Caelen, and Liyun He-Guelton. 2017. Efficient Top Rank Optimization with Gradient Boosting for Supervised Anomaly Detection. In *European Conference on Machine Learning and Knowledge Discovery in Databases*. 20–35.
- [16] Ian J. Goodfellow, Jonathon Shlens, and Christian Szegedy. 2015. Explaining and Harnessing Adversarial Examples. In *International Conference on Learning Representations*.
- [17] Kaiming He, Xiangyu Zhang, Shaoqing Ren, and Jian Sun. 2016. Deep Residual Learning for Image Recognition. In *IEEE Conference on Computer Vision and Pattern Recognition*. 770–778.
- [18] Shu Hu, Lipeng Ke, Xin Wang, and Siwei Lyu. 2021. TkML-AP: Adversarial Attacks to Top- $k$  Multi-Label Learning. In *IEEE/CVF International Conference on Computer Vision*. 7629–7637.
- [19] Shu Hu, Yiming Ying, Xin Wang, and Siwei Lyu. 2020. Learning by Minimizing the Sum of Ranked Range. In *Annual Conference on Neural Information Processing Systems*.
- [20] Mengqi Huang, Zhendong Mao, Penghui Wang, Quan Wang, and Yongdong Zhang. 2022. DSE-GAN: Dynamic Semantic Evolution Generative Adversarial Network for Text-to-Image Generation. In *ACM International Conference on Multimedia*. 4345–4354.
- [21] Di Jin, Zhijing Jin, Joey Tianyi Zhou, and Peter Szolovits. 2020. Is BERT Really Robust? A Strong Baseline for Natural Language Attack on Text Classification and Entailment. In *AAAI Conference on Artificial Intelligence*. 8018–8025.
- [22] Qiyu Kang, Yang Song, Qinxu Ding, and Wee Peng Tay. 2021. Stable Neural ODE with Lyapunov-Stable Equilibrium Points for Defending Against Adversarial Attacks. In *Annual Conference on Neural Information Processing Systems*. 14925–14937.
- [23] Valentin Khrulkov and Ivan V. Oseledets. 2018. Art of Singular Vectors and Universal Adversarial Perturbations. In *IEEE Conference on Computer Vision and Pattern Recognition*.
- [24] Alexey Kurakin, Ian J. Goodfellow, and Samy Bengio. 2017. Adversarial Machine Learning at Scale. In *International Conference on Learning Representations*.
- [25] Maosen Li, Yanhua Yang, Kun Wei, Xu Yang, and Heng Huang. 2022. Learning Universal Adversarial Perturbation by Adversarial Example. In *AAAI Conference on Artificial Intelligence*. 1350–1358.
- [26] Tong Li, Sheng Gao, and Yajing Xu. 2017. Deep Multi-Similarity Hashing for Multi-label Image Retrieval. In *ACM on Conference on Information and Knowledge Management*. 2159–2162.
- [27] Zhaopeng Li, Qianqian Xu, Yangbangyan Jiang, Xiaochun Cao, and Qingming Huang. 2020. Quaternion-Based Knowledge Graph Network for Recommendation. In *ACM International Conference on Multimedia*. 880–888.
- [28] Tsung-Yi Lin, Michael Maire, Serge J. Belongie, James Hays, Pietro Perona, Deva Ramanan, Piotr Dollár, and C. Lawrence Zitnick. 2014. Microsoft COCO: Common Objects in Context. In *European Conference on Computer Vision*. 740–755.
- [29] Ying Lin, Heng Ji, Fei Huang, and Lingfei Wu. 2020. A Joint Neural Model for Information Extraction with Global Features. In *Annual Meeting of the Association for Computational Linguistics*. 7999–8009.
- [30] Hong Liu, Rongrong Ji, Jie Li, Baochang Zhang, Yue Gao, Yongjian Wu, and Feiyue Huang. 2019. Universal Adversarial Perturbation via Prior Driven Uncertainty Approximation. In *IEEE/CVF International Conference on Computer Vision*. 2941–2949.
- [31] Li-Ping Liu, Thomas G. Dietterich, Nan Li, and Zhi-Hua Zhou. 2016. Transductive Optimization of Top  $k$  Precision. In *International Joint Conference on Artificial Intelligence*. 1781–1787.
- [32] Chen Ma, Liheng Ma, Yingxue Zhang, Haolun Wu, Xue Liu, and Mark Coates. 2021. Knowledge-Enhanced Top-K Recommendation in Poincaré Ball. In *AAAI Conference on Artificial Intelligence*. 4285–4293.
- [33] Tim Meinhardt, Alexander Kirillov, Laura Leal-Taixé, and Christoph Feichtenhofer. 2022. TrackFormer: Multi-Object Tracking with Transformers. In *IEEE/CVF Conference on Computer Vision and Pattern Recognition*. 8834–8844.
- [34] Stefano Melacci, Gabriele Ciravegna, Angelo Sotgiu, Ambra Demontis, Battista Biggio, Marco Gori, and Fabio Roli. 2022. Domain Knowledge Alleviates Adversarial Attacks in Multi-Label Classifiers. *IEEE Trans. Pattern Anal. Mach. Intell.* 44, 12 (2022), 9944–9959.
- [35] Trisha Mittal, Uttaran Bhattacharya, Rohan Chandra, Aniket Bera, and Dinesh Manocha. 2020. M3ER: Multiplicative Multimodal Emotion Recognition using Facial, Textual, and Speech Cues. In *AAAI Conference on Artificial Intelligence*. 1359–1367.
- [36] Seyed-Mohsen Moosavi-Dezfooli, Alhussein Fawzi, Omar Fawzi, and Pascal Frossard. 2017. Universal Adversarial Perturbations. In *IEEE Conference on Computer Vision and Pattern Recognition*. 86–94.
- [37] Seyed-Mohsen Moosavi-Dezfooli, Alhussein Fawzi, and Pascal Frossard. 2016. DeepFool: A Simple and Accurate Method to Fool Deep Neural Networks. In *IEEE Conference on Computer Vision and Pattern Recognition*. 2574–2582.
- [38] Włodzimierz Ogryczak and Arie Tamir. 2003. Minimizing the sum of the  $k$  largest functions in linear time. *Inform. Process. Lett.* (2003), 117–122.
- [39] Adam Paszke, Sam Gross, Francisco Massa, Adam Lerer, James Bradbury, Gregory Chanan, Trevor Killeen, Zeming Lin, Natalia Gimeshina, Luca Antiga, Alban Desmaison, Andreas Köpf, Edward Z. Yang, Zachary DeVito, Martin Raison, Alykhan Tejani, Sasank Chilamkurthy, Benoit Steiner, Lu Fang, Junjie Bai, and Soumith Chintala. 2019. PyTorch: An Imperative Style, High-Performance Deep Learning Library. In *Annual Conference on Neural Information Processing Systems*. 8024–8035.
- [40] Liang Qiao, Sanli Tang, Zhanzhan Cheng, Yunlu Xu, Yi Niu, Shiliang Pu, and Fei Wu. 2020. Text Perceptron: Towards End-to-End Arbitrary-Shaped Text Spotting. In *AAAI Conference on Artificial Intelligence*. 11899–11907.
- [41] Tal Ridnik, Emanuel Ben Baruch, Nadav Zamir, Asaf Noy, Itamar Friedman, Matan Protter, and Lihi Zelnik-Manor. 2021. Asymmetric Loss For Multi-Label Classification. In *IEEE/CVF International Conference on Computer Vision*. 82–91.
- [42] Qingquan Song, Haifeng Jin, Xiao Huang, and Xia Hu. 2018. Multi-label Adversarial Perturbations. In *IEEE International Conference on Data Mining*. 1242–1247.
- [43] Gaurang Sriramanan, Sravanti Addepalli, Arya Baburaj, and Venkatesh Babu R. 2020. Guided Adversarial Attack for Evaluating and Enhancing Adversarial Defenses. In *Annual Conference on Neural Information Processing Systems*.
- [44] Ilya Sutskever, James Martens, George E. Dahl, and Geoffrey E. Hinton. 2013. On the importance of initialization and momentum in deep learning. In *International Conference on Machine Learning*. 1139–1147.
- [45] Christian Szegedy, Wojciech Zaremba, Ilya Sutskever, Joan Bruna, Dumitru Erhan, Ian J. Goodfellow, and Rob Fergus. 2014. Intriguing properties of neural networks. In *International Conference on Learning Representations*.
- [46] Nurislam Tursynbek, Aleksandr Petiushko, and Ivan V. Oseledets. 2022. Geometry-Inspired Top- $k$  Adversarial Perturbations. In *IEEE/CVF Winter Conference on Applications of Computer Vision*. 4059–4068.
- [47] Xuan-Son Vu, Duc-Trong Le, Christoffer Edlund, Lili Jiang, and Hoang D. Nguyen. 2020. Privacy-Preserving Visual Content Tagging using Graph Transformer Networks. In *ACM International Conference on Multimedia*. 2299–2307.
- [48] Hao Wang, Pu Lu, Hui Zhang, Mingkun Yang, Xiang Bai, Yongchao Xu, Mengchao He, Yongpan Wang, and Wenyu Liu. 2020. All You Need Is Boundary: Toward Arbitrary-Shaped Text Spotting. In *AAAI Conference on Artificial Intelligence*. 12160–12167.
- [49] Qiang Wang, Li Zhang, Luca Bertinetto, Weiming Hu, and Philip H. S. Torr. 2019. Fast Online Object Tracking and Segmentation: A Unifying Approach. In *IEEE*

- Conference on Computer Vision and Pattern Recognition*. 1328–1338.
- [50] Zhibo Wang, Xiaowei Dong, Henry Xue, Zhifei Zhang, Weifeng Chiu, Tao Wei, and Kui Ren. 2022. Fairness-aware Adversarial Perturbation Towards Bias Mitigation for Deployed Deep Models. In *IEEE/CVF Conference on Computer Vision and Pattern Recognition*. 10369–10378.
- [51] Zeyuan Wang, Chaofeng Sha, and Su Yang. 2021. Reinforcement Learning Based Sparse Black-box Adversarial Attack on Video Recognition Models. In *International Joint Conference on Artificial Intelligence*. 3162–3168.
- [52] Zitai Wang, Qianqian Xu, Zhiyong Yang, Yuan He, Xiaochun Cao, and Qingming Huang. 2023. Optimizing Partial Area Under the Top-k Curve: Theory and Practice. *IEEE Trans. Pattern Anal. Mach. Intell.* 45, 4 (2023), 5053–5069.
- [53] Tong Wei, Zhen Mao, Jiang-Xin Shi, Yu-Feng Li, and Min-Ling Zhang. 2022. A Survey on Extreme Multi-label Learning. *CoRR* abs/2210.03968 (2022).
- [54] Zhipeng Wei, Jingjing Chen, Zuxuan Wu, and Yu-Gang Jiang. 2022. Cross-Modal Transferable Adversarial Attacks from Images to Videos. In *IEEE/CVF Conference on Computer Vision and Pattern Recognition*. 15044–15053.
- [55] Peisong Wen, Qianqian Xu, Zhiyong Yang, Yuan He, and Qingming Huang. 2022. Exploring the Algorithm-Dependent Generalization of AUPRC Optimization with List Stability. In *Annual Conference on Neural Information Processing Systems*.
- [56] Xi-Zhu Wu and Zhi-Hua Zhou. 2017. A Unified View of Multi-Label Performance Measures. In *International Conference on Machine Learning*. 3780–3788.
- [57] Tao Xiang, Hangcheng Liu, Shangwei Guo, Hantao Liu, and Tianwei Zhang. 2022. Text’s Armor: Optimized Local Adversarial Perturbation Against Scene Text Editing Attacks. In *ACM International Conference on Multimedia*. 2777–2785.
- [58] Chaowei Xiao, Bo Li, Jun-Yan Zhu, Warren He, Mingyan Liu, and Dawn Song. 2018. Generating Adversarial Examples with Adversarial Networks. In *International Joint Conference on Artificial Intelligence*. 3905–3911.
- [59] Forest Yang and Sanmi Koyejo. 2020. On the consistency of top-k surrogate losses. In *International Conference on Machine Learning*. 10727–10735.
- [60] Yi Yu, Wenhao Yang, Yap-Peng Tan, and Alex C. Kot. 2022. Towards Robust Rain Removal Against Adversarial Attacks: A Comprehensive Benchmark Analysis and Beyond. In *IEEE/CVF Conference on Computer Vision and Pattern Recognition*. 6003–6012.
- [61] Jiutao Yue, Haofeng Li, Pengxu Wei, Guanbin Li, and Liang Lin. 2021. Robust Real-World Image Super-Resolution against Adversarial Attacks. In *ACM Multimedia Conference*. 5148–5157.
- [62] Chaoning Zhang, Philipp Benz, Tooba Imtiaz, and In So Kweon. 2020. Understanding Adversarial Examples From the Mutual Influence of Images and Perturbations. In *IEEE/CVF Conference on Computer Vision and Pattern Recognition*. 14509–14518.
- [63] Zekun Zhang and Tianfu Wu. 2020. Learning Ordered Top-k Adversarial Attacks via Adversarial Distillation. In *IEEE/CVF Conference on Computer Vision and Pattern Recognition*. 3364–3373.
- [64] Jiawei Zhao, Ke Yan, Yifan Zhao, Xiaowei Guo, Feiyue Huang, and Jia Li. 2021. Transformer-based Dual Relation Graph for Multi-label Image Recognition. In *IEEE/CVF International Conference on Computer Vision*. 163–172.



**Table 5: Summary of well-trained models on different datasets.**

Dataset	VOC 2012	COCO 2014	NUS WIDE
Backbone	ResNet-50	ResNet-101	ResNet-101
Input size	300	448	224
Optimizer	SGD	Adam	Adam
Batch size	32	128	64
Learning rate	1e-4	1e-4	1e-4
Weight decay	1e-4	1e-4	1e-4
mAP	0.949	0.906	0.828

## A PROOFS

### A.1 Proof of Lemma 4.1

LEMMA 4.1 ([38]). For  $\lambda \in [0, 1]$ ,  $f_i(\mathbf{x}) \in [0, 1]$ ,  $i = 1, \dots, c$ , we have

$$\sum_{i=1}^k f_{[i]}(\mathbf{x}) = \min_{\lambda \in [0, 1]} \left\{ k\lambda + \sum_{i=1}^c [f_i(\mathbf{x}) - \lambda]_+ \right\},$$

where  $[a]_+ = \max\{0, a\}$ , and  $f_{[k]}(\mathbf{x})$  is one optimal solution.

PROOF. We first define  $\mathbf{p}$  as a coefficient vector with size  $c$ , whose component is denoted as  $p_i$ . It is noted that  $\sum_{i=1}^k f_{[i]}(\mathbf{x})$  is the solution of the following programming problem:

$$\max_{\mathbf{p}} \mathbf{p}^\top \mathbf{F}, \quad \text{s.t. } \mathbf{p}^\top \mathbf{1} = k, \quad 0 \leq p_i \leq 1, \quad i = 1, \dots, c. \quad (14)$$

To solve this problem, we could utilize the Lagrangian equation, converting Eq.(14) to

$$L(\mathbf{p}, \mathbf{u}, \mathbf{v}, \lambda) = -\mathbf{p}^\top \mathbf{F} - \mathbf{u}^\top \mathbf{p} + \mathbf{v}^\top (\mathbf{p} - \mathbf{1}) + \lambda(\mathbf{p}^\top \mathbf{1} - k),$$

where non-negative vectors  $\mathbf{u}$ ,  $\mathbf{v}$ , and  $\lambda \in \mathbb{R}$  are Lagrangian multipliers. Let us take its derivative w.r.t  $\mathbf{p}$  and set it to be  $\mathbf{0}$ , we obtain  $\mathbf{v} = \mathbf{u} - \mathbf{F} + \lambda \mathbf{1}$ . According to this equation, we further get the dual problem of the original problem by substituting it into Eq.(14):

$$\min_{\mathbf{u}, \lambda} \mathbf{u}^\top \mathbf{1} + k\lambda, \quad \text{s.t. } \mathbf{u} \geq \mathbf{0}, \mathbf{u} - \mathbf{F} + \lambda \mathbf{1} \geq \mathbf{0}.$$

Due to  $\mathbf{u} \geq \mathbf{F} - \lambda \mathbf{1} \geq \mathbf{0}$ , it is easy to know  $\lambda \in [0, 1]$ , and we thus obtain the final equivalent form:

$$\sum_{i=1}^k f_{[i]}(\mathbf{x}) = \min_{\lambda \in [0, 1]} \left\{ k\lambda + \sum_{i=1}^c [f_i(\mathbf{x}) - \lambda]_+ \right\}. \quad (15)$$

Through Eq.(15), we observe  $f_{[k]}(\mathbf{x})$  is always an optimal solution, i.e.

$$f_{[k]}(\mathbf{x}) \in \min_{\lambda \in [0, 1]} \left\{ k\lambda + \sum_{i=1}^c [f_i(\mathbf{x}) - \lambda]_+ \right\}. \quad (16)$$

□

### A.2 Proof of Lemma 4.2

LEMMA 4.2 ([14]). For  $\forall a > 0, b > 0$ , we have  $[[a - x]_+ - b]_+ = [a - x - b]_+$ .

PROOF. Denote  $g(x) = [[a - x]_+ - b]_+$ . For any  $a \geq 0, b \geq 0$ , we have  $g(x) = 0 = [a - b - x]_+$  when  $a \leq x$ . In the case of  $a > x$ , there holds  $g(x) = [a - b - x]_+$ . Thus  $g(x) = [[a - x]_+ - b]_+ = [a - b - x]_+$  holds for any  $a \geq 0, b \geq 0$ . □

## B MORE EXPERIMENTAL DETAILS

### B.1 Datasets Information

We carry out our experiments on three well-known benchmark multi-label image annotation datasets:

- **PASCAL VOC 2012** (VOC) [13] is a widely used dataset for evaluating the performance of multi-label models toward computer vision tasks. It consists of 10K images with 20 different categories. The dataset is divided into a training set with 5,011 images and a validation set with 4,952 images, respectively. Each image within the training set contains on average 1.43 relevant labels but no more than 6.
- **MS COCO 2014** (COCO) [28] is another multimedia large-scale dataset that contains 122,218 annotation images with 80 object categories and the corresponding descriptions. These images are divided into two parts, where 82,081 images are for training and 40,137 images are for validation. Each image within the training set contains on average 2.9 labels and a maximum of 13 labels.
- **NUS WIDE** (NUS) [9] is a common dataset consisting of 269,648 real-world web images, where some images are obtained from multimedia data. It covers 81 dedicated categories and each image contains on average 2.4 associated labels. We exclude the images without any labels and randomly divided them into two parts. Specifically, there are 103,990 images in the training set and 69,706 images in the test set.

### B.2 Competitors Introductions

The details about our comparison methods are shown as follows:

- $T_k$ ML-AP-U [18]. This is the first top- $k$  untargeted attack method for producing multi-label adversarial perturbation, which is the main baseline to compare with our method.
- $k$ Fool [46]. Inspired by the traditional method DeepFool [37], this method is proposed to generate the top- $k$  adversarial perturbation in multi-class classification. To apply to multi-label learning, we consider its prediction score for the only relevant label as the maximum score among all relevant labels like [18].
- ML-CW-U. We adopt a similar untargeted vision of C&W [5] as our comparison method, which adopts the loss function  $[\max_{i \notin Y_p} f_i(\mathbf{x} + \epsilon) - \min_{j \in Y_p} f_j(\mathbf{x} + \epsilon)]_+$ . Compared to  $CW^k$ , this method simply extends C&W to multi-label adversarial learning while not considering the order factor.

### B.3 Model Details

Table 5 summarizes the parameters and mAP results of the well-trained models used on each dataset, where the momentum for SGD is empirically set as 0.9. Both ResNet-50 and ResNet-101 are pre-trained on ImageNet [10]. Utilizing the binary cross-entropy loss, we further fine-tune the model to fit the classification task on different datasets.

**Table 8: Correspondence between types and categories on NUS.**

Type	Categories
Animals	elk, bear, cat, zebra, fish,
	whales, dog, cow, horse, fox,
Buildings	birds, tiger, animal.
	bridge, statue, tower, temple,
	buildings, house, castle.
Landscape	waterfall, rainbow, lake, sunset,
	moon, ocean, beach, town,
	glacier, sun, clouds, valley,
	cityscape, frost, sky, harbor, garden,
Traffic	earthquake, surf, mountain, nighttime.
	plane, airport, train, boats,
	cars, road, vehicle, street, railroad.

**Table 9: Number of samples under different types and  $k$  values on VOC.**

Type	$k$	$ S $	$n$
Vehicles	1	1.0000	365
	2	1.0384	26
	3	1.0000	6
Animals	1	1.0000	213
	2	1.0000	45
	3	1.0000	7
Household	1	1.0000	120
	2	1.0000	28
	3	1.0000	1
Person	1	1.0000	888
	2	1.0000	319
	3	1.0000	59

**Table 10: Number of samples under different types and  $k$  values on COCO.**

Type	$k$	$ S $	$n$
Person	3	1.0000	1000
	5	1.0000	1000
	10	1.0000	82
Daily necessities	3	1.0700	1000
	5	1.1089	790
	10	1.1666	30
Furniture	3	1.1519	1000
	5	1.3539	1000
	10	1.7555	45
Electrical equipment	3	1.2130	1000
	5	1.3091	702
	10	1.3478	23

**Table 11: Number of samples under different types and  $k$  values on NUS.**

Type	$k$	$ S $	$n$
Animals	2	1.2710	1000
	3	1.2203	590
	5	1.1818	66
Buildings	2	1.0080	1000
	3	1.0250	1000
	5	1.0636	535
Landscape	2	1.2940	1000
	3	1.4340	1000
	5	1.7027	259
Traffic	2	1.1150	1000
	3	1.0849	860
	5	1.0588	255

#### B.4 Category Description

For the experiments under the global selection scheme on VOC, COCO, and NUS, we present the specified categories included in each type in Table 6, Table 7 and Table 8, respectively. We select various scales of specified label sets to better show the performance of our method under different parameters.

**Table 6: Correspondence between types and categories on VOC.**

Type	Categories
Vehicles	bird, cat, cow, dog, horse, sheep.
Animals	aeroplane, bicycle, boat, bus,
	car, motorbike, train.
Household	bottle, chair, dining table,
	potted plant, sofa, TV monitor.
Person	person.

**Table 7: Correspondence between types and categories on COCO.**

Type	Categories
Person	person.
Daily necessities	backpack, umbrella, handbag, tie,
	suitcase, book, clock, vase,
	scissors, teddy bear, toothbrush.
Furniture	chair, couch, potted plant,
	bed, dining table.
Electrical equipment	TV, laptop, mouse, remote,
	keyboard, cell phone, microwave,
	oven, toaster, refrigerator.

**Table 12: Number of samples under random selection scheme.**

Dataset	$k$	$ S $	$n$
VOC	2	2	69
	3	3	11
COCO	3	2	1000
		3	1000
		2	1000
	5	3	1000
		5	206
		2	63
	10	3	21
		5	2
NUS	2	2	1000
	3	2	1000
		3	1000
		2	1000
	5	3	559
		5	24

## B.5 Number of Samples under Different Settings

As the selected samples have to satisfy  $|Y_p| \geq k + |S|$ , the number of samples under various settings is different. Thus, we present the specific numbers of samples and their average specified labels under different settings in Table 9–12. In particular, Table 9, Table 10, and Table 11 show the correspondence under the global selection scheme on each dataset, respectively. And Table 12 integrates the number of samples on different datasets under the random selection scheme. Please note that we only select up to 1000 samples as our test images for each experiment.

## C ADDITIONAL RESULTS AND ANALYSIS

### C.1 Overall Performance under Scheme 1

The overall performance of  $T_k$ MIA and other methods under the global selection scheme on COCO, NUS, and VOC are shown in Table 13, Table 14, and Table 15, respectively.

We can clearly see that our method completely outperforms the other comparison methods. Specifically, our method could generate smaller perturbations to achieve a slight change in metrics. Meanwhile, we obtain a larger  $\Delta I$ , which means that our approach successfully perturbs more specified categories. On one hand, we could observe that all methods generate larger perturbations with increasing the  $k$  value while the increase in our average perturbation norm is smaller than others. For example, on the Traffic type of NUS, when  $k$  changes from 2 to 5, the APer of ML-CW-U,  $k$ Fool, and  $T_k$ ML-AP-U increase 0.7295, 5.4391, and 0.6772, respectively. Our  $T_k$ MIA only produces 0.0934 increasing. For some types (Vehicles, Animals, Household types of VOC), its APer even produces a decreasing trend. On the other hand, most changes in measures for all methods get smaller as the  $k$  value increases. But when there are large  $k$  and  $|S|$ ,  $T_k$ ML-AP-U yields the opposite trend, such as on Daily necessities and Furniture types of COCO. This comparison indicates that our method is more robust in complex conditions.

Through these two aspects, we verify the outstanding performance of our method.

### C.2 Overall Performance under Scheme 2

In the main paper, we only present the performance of different methods under Scheme 2 with the maximum iteration of 300 and  $\delta = 2$  on NUS. In this part, Table 16 to Table 23 present the overall performance of different methods under various parameters on three datasets in the random selection scheme, where the maximum iteration ranges from  $\{100, 300, 500\}$  and  $\delta = 2, 3$ .

From the results on VOC and COCO, we could more intuitively find the superiority of our method. But for the results on NUS, which are shown in Table 21–23, the  $\Delta I$  and APer values of our perturbation are not the best. We think there are two possible reasons. The first one is that since the model training on NUS can only achieve 0.828 mAP which is shown in Table 5, its original classification effect is relatively poor. This means there exist more irrelevant labels in the top- $k$  set. To satisfy measure imperceptibility, the model needs to take more effort to push them outside the top- $k$  position; (2) as our perturbation is required to achieve both visual and measure imperceptibility, it has to make a trade-off between the perturbed number and perturbation size in some cases. We could see that  $k$ Fool usually presents a better average attack effectiveness while generating an obvious perturbation, and  $T_k$ ML-AP-U makes a smaller APer but overlook the impact on metrics. In contrast, our  $T_k$ MIA could achieve both properties and avoid these problems. Therefore, these results and analyses further validate the effectiveness of our perturbation and optimization framework.

### C.3 Visualization Results

We set the maximum iteration as 300 and  $\delta = 2$  to present the image results under Scheme 1 and Scheme 2 from Figure 4 to Figure 7, where the first two sets of images are the performance on VOC and the others are on COCO.

In Figure 4, we see that for our method, the metrics of the perturbed image remain unchanged. While other methods produce a clear performance degradation that causes a significant change in metrics. In Figure 5, it is not hard to find that even if all methods achieve the ideal results, our perturbation could craft a smaller perturbation to lower the ranking position of specified labels. Hence, the overall performance of our method demonstrates that the proposed perturbation is more effective than other attacks when pursuing both visual and measure imperceptibility.

From the results on COCO, we could find that our perturbation manage to push the specified categories out of the top- $k$  region with slight efforts. Meanwhile, its changes in ranking-based metric values could be almost ignored, which achieves our perturbation effect. For  $k$ Fool, its perturbations always make the perturbed images visually perceptible though it could fool all metrics in some cases. Although  $T_k$ ML-AP-U performs well in some images, its overall effect is not better than our perturbation. This is consistent with our analysis shown in Sec.5.2.

**Table 13: The rest results of competitors and our method with the maximum iteration 300 under different  $k$  values and globally selected  $S$  on COCO, where  $\Delta$  refers to the difference between the original value and the perturbed value of corresponding metrics.  $\downarrow$  means the smaller the value the better, and  $\uparrow$  is the opposite. The best results under each set of parameters are bolded.**

Type	$k$	Methods	$\Delta T_k \text{Acc} \downarrow$	$\Delta P@k \downarrow$	$\Delta mAP@k \downarrow$	$\Delta NDCG@k \downarrow$	$\Delta I \uparrow$	APer $\downarrow$
Daily necessities	3	ML-CW-U	0.6040	0.3200	0.4015	0.3303	1.0690	1.4187
		kFool	0.6110	0.3613	0.4047	0.3350	0.8170	13.5042
		$T_k$ ML-AP-U	0.6060	0.3213	0.4112	0.3401	1.0700	1.1906
		$T_k$ MIA(Ours)	<b>0.2660</b>	<b>0.1163</b>	<b>0.1280</b>	<b>0.0958</b>	<b>1.0700</b>	<b>0.5063</b>
	5	ML-CW-U	0.4474	0.3534	0.4857	0.4168	1.1077	1.6318
		kFool	0.4246	0.3194	0.3845	0.3119	1.0139	18.3515
		$T_k$ ML-AP-U	0.4397	0.3333	0.4672	0.4017	1.1077	1.3634
		$T_k$ MIA(Ours)	<b>0.1825</b>	<b>0.0884</b>	<b>0.1022</b>	<b>0.0729</b>	<b>1.1089</b>	<b>0.5418</b>
	10	ML-CW-U	0.0000	0.3367	0.4756	0.4389	1.1666	1.9130
		kFool	0.0333	0.2433	0.3237	0.2697	0.9333	23.1311
		$T_k$ ML-AP-U	0.0000	0.3533	0.4905	0.4571	1.1666	1.6887
		$T_k$ MIA(Ours)	<b>0.0000</b>	<b>0.0433</b>	<b>0.0605</b>	<b>0.0384</b>	<b>1.1666</b>	<b>0.5724</b>
Furniture	3	ML-CW-U	0.6270	0.3497	0.4509	0.3806	1.1510	1.2603
		kFool	0.5960	0.3467	0.3972	0.3300	0.6430	12.7266
		$T_k$ ML-AP-U	0.5990	0.3383	0.4437	0.3755	1.1519	1.0673
		$T_k$ MIA(Ours)	<b>0.3210</b>	<b>0.1446</b>	<b>0.1605</b>	<b>0.1221</b>	<b>1.1519</b>	<b>0.4519</b>
	5	ML-CW-U	0.4970	0.3970	0.5421	0.4710	1.3540	1.7799
		kFool	0.4800	0.3800	0.4684	0.3920	0.8240	53.0367
		$T_k$ ML-AP-U	0.4860	0.3964	0.5515	0.4821	1.3539	1.5302
		$T_k$ MIA(Ours)	<b>0.2490</b>	<b>0.1286</b>	<b>0.1513</b>	<b>0.1105</b>	<b>1.3539</b>	<b>0.7216</b>
	10	ML-CW-U	0.1333	0.3933	0.5712	0.5152	1.7333	2.1470
		kFool	0.1333	0.2933	0.4121	0.3296	0.7333	97.2627
		$T_k$ ML-AP-U	0.1333	0.4333	0.6065	0.5514	1.7333	1.9629
		$T_k$ MIA(Ours)	<b>0.0444</b>	<b>0.1133</b>	<b>0.1291</b>	<b>0.0891</b>	<b>1.7555</b>	<b>0.9502</b>
Electrical equipment	3	ML-CW-U	0.5810	0.3323	0.4159	0.3508	1.2130	0.9664
		kFool	0.5730	0.3267	0.3798	0.3149	0.9040	12.5737
		$T_k$ ML-AP-U	0.5580	0.3126	0.4018	0.3372	1.2130	0.7998
		$T_k$ MIA(Ours)	<b>0.3330</b>	<b>0.1600</b>	<b>0.1758</b>	<b>0.1360</b>	<b>1.2130</b>	<b>0.4253</b>
	5	ML-CW-U	0.3647	0.2786	0.4063	0.3437	1.3077	1.2748
		kFool	0.3818	0.2823	0.3612	0.2886	0.9829	14.8029
		$T_k$ ML-AP-U	0.3589	0.2695	0.3981	0.3368	1.3091	1.0406
		$T_k$ MIA(Ours)	<b>0.2136</b>	<b>0.1128</b>	<b>0.1360</b>	<b>0.0985</b>	<b>1.3091</b>	<b>0.4702</b>
	10	ML-CW-U	0.0000	0.2652	0.4097	0.3546	1.3478	1.6874
		kFool	0.0000	0.1826	0.2591	0.1874	1.0435	8.7268
		$T_k$ ML-AP-U	0.0000	0.2086	0.3510	0.2944	1.3478	1.3869
		$T_k$ MIA(Ours)	<b>-0.0434</b>	<b>0.0608</b>	<b>0.0914</b>	<b>0.0679</b>	<b>1.3478</b>	<b>0.5378</b>

**Table 14: The rest results of competitors and our method with the maximum iteration 300 under different  $k$  values and globally selected  $S$  on NUS, where  $\Delta$  refers to the difference between the original value and the perturbed value of corresponding metrics.  $\downarrow$  means the smaller the value the better, and  $\uparrow$  is the opposite. The best results under each set of parameters are bolded.**

Type	$k$	Methods	$\Delta T_k \text{Acc} \downarrow$	$\Delta P@k \downarrow$	$\Delta mAP@k \downarrow$	$\Delta \text{NDCG}@k \downarrow$	$\Delta I \uparrow$	APer $\downarrow$
Animals	2	ML-CW-U	0.4240	0.2545	0.3043	0.2612	1.2600	1.2388
		$k$ Fool	0.4080	0.2465	0.2755	0.2362	1.1290	5.1962
		$T_k$ ML-AP-U	0.4290	0.2585	0.3135	0.2697	1.2649	1.1038
		$T_k$ MIA(Ours)	<b>0.2410</b>	<b>0.1485</b>	<b>0.1715</b>	<b>0.1484</b>	<b>1.2710</b>	<b>0.9219</b>
	3	ML-CW-U	0.4288	0.2373	0.3096	0.2568	1.1712	1.4019
		$k$ Fool	0.4136	0.2508	0.2702	0.2222	1.0339	5.8748
		$T_k$ ML-AP-U	0.4470	0.2485	0.3282	0.2741	1.1847	1.2732
		$T_k$ MIA(Ours)	<b>0.1966</b>	<b>0.1040</b>	<b>0.1195</b>	<b>0.0961</b>	<b>1.2203</b>	<b>0.8284</b>
	5	ML-CW-U	0.3788	0.2000	0.2684	0.2184	0.9697	1.5046
		$k$ Fool	0.2879	0.2424	0.2702	0.2236	0.9848	10.4123
		$T_k$ ML-AP-U	0.3484	0.2121	0.3098	0.2588	0.9545	1.4826
		$T_k$ MIA(Ours)	<b>0.1364</b>	<b>0.0424</b>	<b>0.0498</b>	<b>0.0367</b>	<b>1.1818</b>	<b>0.7242</b>
Landscape	2	ML-CW-U	0.6160	0.4250	0.5113	0.4598	1.2150	1.8080
		$k$ Fool	0.6770	0.4985	0.5273	0.4841	1.2160	36.0644
		$T_k$ ML-AP-U	0.6310	0.4405	0.5313	0.4795	1.2569	1.4559
		$T_k$ MIA(Ours)	<b>0.1300</b>	<b>0.0910</b>	<b>0.0993</b>	<b>0.0896</b>	<b>1.2940</b>	<b>1.0430</b>
	3	ML-CW-U	0.5660	0.3900	0.5130	0.4537	1.2350	2.2045
		$k$ Fool	0.6200	0.4800	0.5141	0.4694	1.3130	70.4729
		$T_k$ ML-AP-U	0.5770	0.4016	0.5337	0.4734	1.3179	1.8304
		$T_k$ MIA(Ours)	<b>0.0770</b>	<b>0.0520</b>	<b>0.0630</b>	<b>0.0537</b>	<b>1.4260</b>	<b>1.3236</b>
	5	ML-CW-U	0.3205	0.2873	0.4037	0.3605	1.0811	2.4561
		$k$ Fool	0.4363	0.4865	0.5635	0.5044	1.4131	159.2512
		$T_k$ ML-AP-U	0.3359	0.3220	0.4665	0.4200	1.2548	2.1796
		$T_k$ MIA(Ours)	<b>-0.0502</b>	<b>0.0232</b>	<b>0.0385</b>	<b>0.0337</b>	<b>1.6525</b>	<b>1.7653</b>
Traffic	2	ML-CW-U	0.3750	0.2360	0.2773	0.2419	1.0970	0.9301
		$k$ Fool	0.4680	0.3485	0.3743	0.3448	1.0950	9.1090
		$T_k$ ML-AP-U	0.3830	0.2405	0.2850	0.2485	1.1060	0.7939
		$T_k$ MIA(Ours)	<b>0.2420</b>	<b>0.1530</b>	<b>0.1705</b>	<b>0.1487</b>	<b>1.1150</b>	<b>0.5297</b>
	3	ML-CW-U	0.4669	0.2455	0.3100	0.2576	1.0128	1.3553
		$k$ Fool	0.5395	0.3946	0.4326	0.3875	1.0779	9.5689
		$T_k$ ML-AP-U	0.4698	0.2469	0.3154	0.2622	1.0326	1.1458
		$T_k$ MIA(Ours)	<b>0.2500</b>	<b>0.1213</b>	<b>0.1337</b>	<b>0.1059</b>	<b>1.0849</b>	<b>0.5889</b>
	5	ML-CW-U	0.3843	0.2047	0.2812	0.2283	0.8235	1.6596
		$k$ Fool	0.4471	0.3867	0.4279	0.4279	1.0510	14.5481
		$T_k$ ML-AP-U	0.3608	0.2125	0.2944	0.2435	0.8902	1.4711
		$T_k$ MIA(Ours)	<b>0.1725</b>	<b>0.0816</b>	<b>0.0863</b>	<b>0.0612</b>	<b>1.0588</b>	<b>0.6231</b>

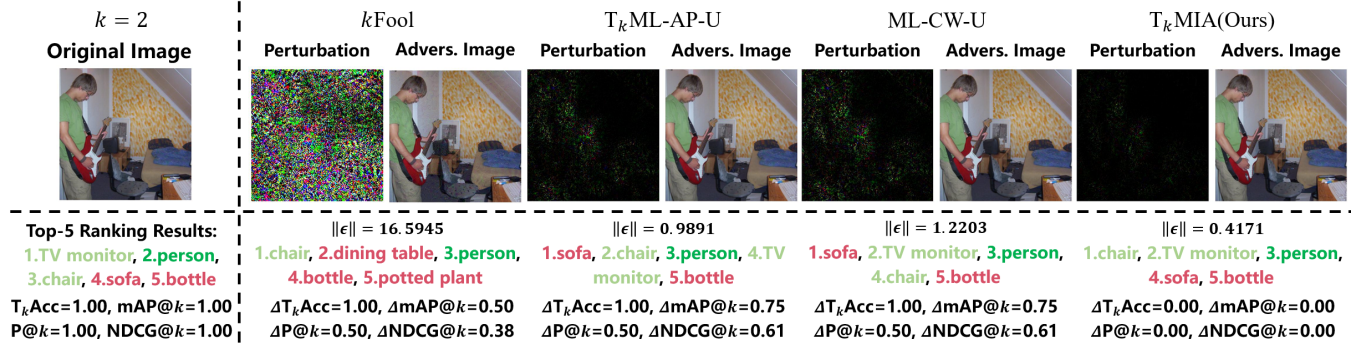


Figure 4: The top-2 successful performance comparisons under *global selection scheme* on VOC, where the maximum iteration is 300. All perturbation intensities are magnified by a factor of 100 to enhance contrast and visibility. The specified labels, relevant labels, and irrelevant labels are marked with dark green, light green, and red, respectively.

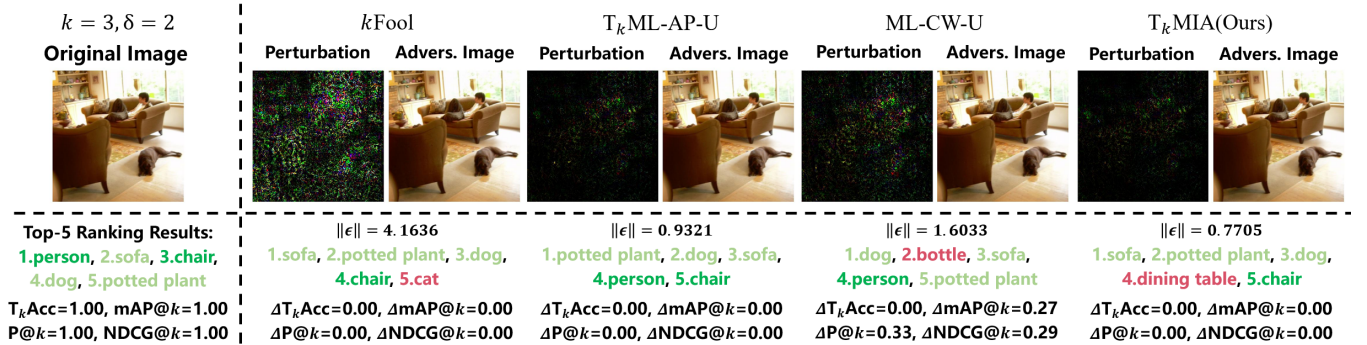


Figure 5: The top-3 successful performance comparisons under *random selection scheme* on VOC, where the maximum iteration is 300. All perturbation intensities are magnified by a factor of 100 to enhance contrast and visibility. The specified labels, relevant labels, and irrelevant labels are marked with dark green, light green, and red, respectively.

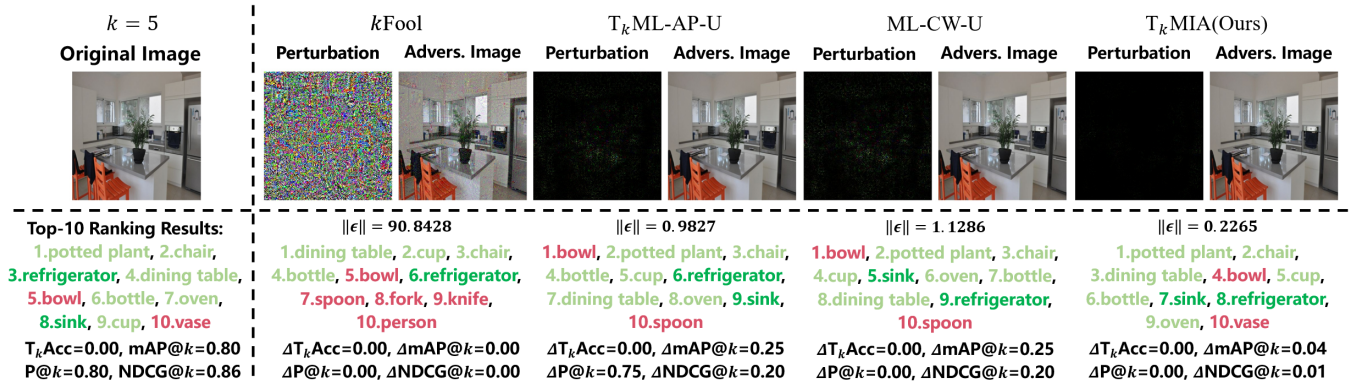


Figure 6: The top-5 successful performance comparisons under *global selection scheme* on COCO, where the maximum iteration is 300. All perturbation intensities are magnified by a factor of 100 to enhance contrast and visibility. The specified labels, relevant labels, and irrelevant labels are marked with dark green, light green, and red, respectively.



**Table 15: The results of competitors and our method with the maximum iteration 300 under different  $k$  values and globally selected  $S$  on VOC, where  $\Delta$  refers to the difference between the original value and the perturbed value of corresponding metrics.  $\downarrow$  means the smaller the value the better, and  $\uparrow$  is the opposite. The best results under each set of parameters are bolded.**

Type	$k$	Methods	$\Delta T_k \text{Acc} \downarrow$	$\Delta P@k \downarrow$	$\Delta mAP@k \downarrow$	$\Delta NDCG@k \downarrow$	$\Delta I \uparrow$	APer $\downarrow$
Vehicles	1	ML-CW-U	0.3452	0.3452	0.3452	0.3452	1.0000	1.0053
		$k$ Fool	0.1978	0.1978	0.1978	0.1978	0.9973	1.8162
		$T_k$ ML-AP-U	0.3489	0.3489	0.3489	0.3489	1.0000	0.8861
		$T_k$ MIA(Ours)	<b>0.1698</b>	<b>0.1698</b>	<b>0.1698</b>	<b>0.1698</b>	<b>1.0000</b>	<b>0.7644</b>
	2	ML-CW-U	0.4615	0.2308	0.3173	0.2569	1.0000	1.7331
		$k$ Fool	0.6923	0.3846	0.4519	0.3759	0.8846	23.1394
		$T_k$ ML-AP-U	0.5000	0.2500	0.3365	0.2717	1.0384	1.4915
		$T_k$ MIA(Ours)	<b>0.1538</b>	<b>0.0769</b>	<b>0.0769</b>	<b>0.0595</b>	<b>1.0384</b>	<b>0.9265</b>
	3	ML-CW-U	0.5000	0.2778	0.4352	0.3622	1.0000	1.3096
		$k$ Fool	0.5000	0.4444	0.4630	0.4218	1.0000	23.3179
		$T_k$ ML-AP-U	0.5000	0.2222	0.3425	0.2737	1.0000	1.1204
		$T_k$ MIA(Ours)	<b>0.1666</b>	<b>0.1111</b>	<b>0.1111</b>	<b>0.0884</b>	<b>1.0000</b>	<b>0.4735</b>
Animals	1	ML-CW-U	0.3333	0.3333	0.3333	0.3333	1.0000	0.7220
		$k$ Fool	0.2639	0.2639	0.2639	0.2639	1.0000	<b>0.5135</b>
		$T_k$ ML-AP-U	0.3287	0.3287	0.3287	0.3287	1.0000	0.6297
		$T_k$ MIA(Ours)	<b>0.1851</b>	<b>0.1851</b>	<b>0.1851</b>	<b>0.1851</b>	<b>1.0000</b>	0.5758
	2	ML-CW-U	0.5556	0.3111	0.4056	0.3413	1.0000	1.3934
		$k$ Fool	0.6000	0.4000	0.4278	0.3799	0.9111	4.3568
		$T_k$ ML-AP-U	0.5333	0.3222	0.4055	0.3498	1.0000	1.1133
		$T_k$ MIA(Ours)	<b>0.1555</b>	<b>0.0777</b>	<b>0.0777</b>	<b>0.0601</b>	<b>1.0000</b>	<b>0.6988</b>
	3	ML-CW-U	0.4286	0.1429	0.2619	0.2011	1.0000	1.1452
		$k$ Fool	0.4286	0.4286	0.4286	0.3791	1.0000	8.2682
		$T_k$ ML-AP-U	0.5714	0.2857	0.4206	0.3439	1.0000	1.1069
		$T_k$ MIA(Ours)	<b>0.1428</b>	<b>0.0952</b>	<b>0.1111</b>	<b>0.0845</b>	<b>1.0000</b>	<b>0.3470</b>
Household	1	ML-CW-U	0.2500	0.2500	0.2500	0.2500	0.9333	0.4442
		$k$ Fool	0.2750	0.2750	0.2750	0.2750	0.9500	1.3002
		$T_k$ ML-AP-U	0.2833	0.2833	0.2833	0.2833	1.0000	0.5046
		$T_k$ MIA(Ours)	<b>0.1583</b>	<b>0.1583</b>	<b>0.1583</b>	<b>0.1583</b>	<b>1.0000</b>	<b>0.4421</b>
	2	ML-CW-U	0.6071	0.3393	0.4375	0.3676	1.0000	1.6331
		$k$ Fool	0.5714	0.3571	0.3929	0.3410	0.4286	9.2461
		$T_k$ ML-AP-U	0.4642	0.2857	0.3571	0.3099	1.0000	1.2804
		$T_k$ MIA(Ours)	<b>0.2142</b>	<b>0.1250</b>	<b>0.1339</b>	<b>0.1128</b>	<b>1.0000</b>	<b>0.5842</b>
	3	ML-CW-U	1.0000	0.6667	0.8333	0.7039	1.0000	2.9472
		$k$ Fool	1.0000	0.6667	0.6667	0.5307	1.0000	6.6913
		$T_k$ ML-AP-U	1.0000	0.6666	0.6666	0.5307	1.0000	2.3044
		$T_k$ MIA(Ours)	<b>1.0000</b>	<b>0.3333</b>	<b>0.3333</b>	<b>0.2346</b>	<b>1.0000</b>	<b>0.2817</b>
Person	1	ML-CW-U	0.3288	0.3288	0.3288	0.3288	0.9955	1.0851
		$k$ Fool	0.2568	0.2568	0.2568	0.2568	1.0000	<b>0.5595</b>
		$T_k$ ML-AP-U	0.3063	0.3063	0.3063	0.3063	0.9966	0.9056
		$T_k$ MIA(Ours)	<b>0.1182</b>	<b>0.1182</b>	<b>0.1182</b>	<b>0.1182</b>	<b>1.0000</b>	0.7834
	2	ML-CW-U	0.5204	0.3056	0.4130	0.3542	0.9875	1.7190
		$k$ Fool	0.4013	0.2414	0.2712	0.2322	0.8307	5.6123
		$T_k$ ML-AP-U	0.4984	0.3009	0.3957	0.3420	1.0000	1.4489
		$T_k$ MIA(Ours)	<b>0.0721</b>	<b>0.0454</b>	<b>0.0595</b>	<b>0.0521</b>	<b>1.0000</b>	<b>1.1268</b>
	3	ML-CW-U	0.4576	0.2542	0.3964	0.3325	1.0000	1.8746
		$k$ Fool	0.3559	0.1808	0.2015	0.1557	0.8305	3.8721
		$T_k$ ML-AP-U	0.4406	0.2485	0.3926	0.3306	0.9491	1.6421
		$T_k$ MIA(Ours)	<b>-0.0338</b>	<b>0.0169</b>	<b>0.0348</b>	<b>0.0311</b>	<b>1.0000</b>	<b>1.2935</b>

**Table 16: The results of competitors and our method with the maximum iteration 100 and  $\delta = 2$  on VOC under different  $k$  values and sizes of randomly selected  $S$ , where  $\Delta$  refers to the difference between the original value and the perturbed value of corresponding metrics.  $\downarrow$  means the smaller the value the better, and  $\uparrow$  is the opposite. The best results under each set of parameters are bolded.**

$k$	$ S $	Methods	$\Delta T_k \text{Acc} \downarrow$	$\Delta P@k \downarrow$	$\Delta mAP@k \downarrow$	$\Delta NDCG@k \downarrow$	$\Delta I \uparrow$	APer $\downarrow$
2	2	ML-CW-U	0.5072	0.3043	0.4022	0.3470	1.3478	1.4079
		$k$ Fool	0.5507	0.3188	0.3478	0.2926	1.4492	12.2294
		$T_k$ ML-AP-U	0.5652	0.3913	0.4673	0.4208	1.5797	<b>1.2688</b>
		$T_k$ MIA(Ours)	<b>0.3043</b>	<b>0.2028</b>	<b>0.2246</b>	<b>0.1996</b>	<b>1.9855</b>	1.4456
3	2	ML-CW-U	0.1818	0.1212	0.2273	0.1976	1.4545	1.3738
		$k$ Fool	0.1818	0.1212	0.1565	0.1335	1.0000	25.7817
		$T_k$ ML-AP-U	1.4545	1.1405	0.0909	0.0909	0.1666	<b>0.1493</b>
		$T_k$ MIA(Ours)	<b>0.0000</b>	<b>0.0606</b>	<b>0.0707</b>	<b>0.0695</b>	<b>2.0000</b>	1.2743

**Table 17: The results of competitors and our method with the maximum iteration 300 and  $\delta = 2$  on VOC under different  $k$  values and sizes of randomly selected  $S$ , where  $\Delta$  refers to the difference between the original value and the perturbed value of corresponding metrics.  $\downarrow$  means the smaller the value the better, and  $\uparrow$  is the opposite. The best results under each set of parameters are bolded.**

$k$	$ S $	Methods	$\Delta T_k \text{Acc} \downarrow$	$\Delta P@k \downarrow$	$\Delta mAP@k \downarrow$	$\Delta NDCG@k \downarrow$	$\Delta I \uparrow$	APer $\downarrow$
2	2	ML-CW-U	0.7101	0.4638	0.5688	0.5031	1.9130	1.8886
		$k$ Fool	0.5507	0.3478	0.3768	0.3281	1.5072	17.3492
		$T_k$ ML-AP-U	0.6956	0.4782	0.5688	0.5110	1.9420	1.5410
		$T_k$ MIA(Ours)	<b>0.2898</b>	<b>0.1956</b>	<b>0.2246</b>	<b>0.2005</b>	<b>2.0000</b>	<b>1.4626</b>
3	2	ML-CW-U	0.3636	0.1818	0.3333	0.2773	1.8182	1.8550
		$k$ Fool	0.1818	0.1212	0.1414	0.1178	1.0909	27.6438
		$T_k$ ML-AP-U	0.3636	0.1818	0.3181	0.2615	2.0000	1.6427
		$T_k$ MIA(Ours)	<b>0.0000</b>	<b>0.0606</b>	<b>0.0707</b>	<b>0.0695</b>	<b>2.0000</b>	<b>1.2769</b>

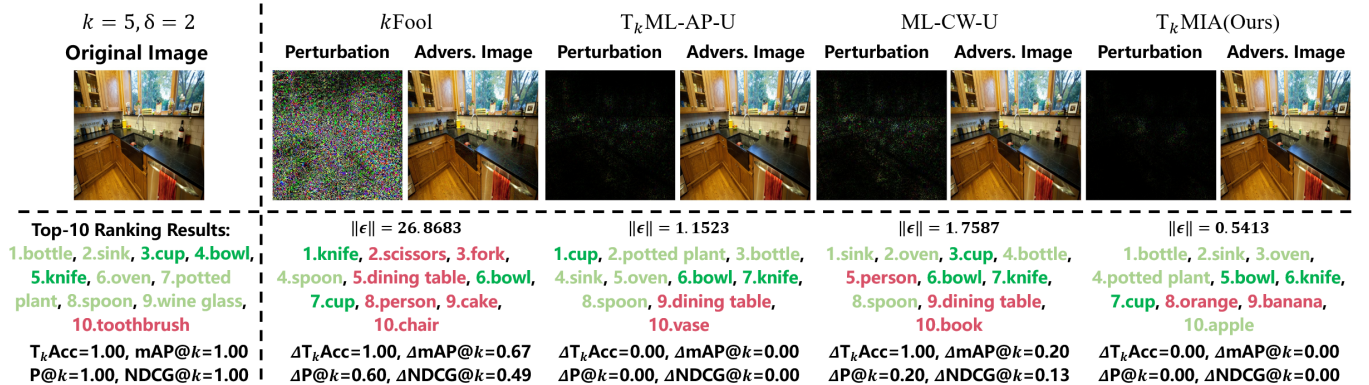


**Figure 7: The top-5 successful performance comparisons under random selection scheme on COCO, where the maximum iteration is 300. All perturbation intensities are magnified by a factor of 100 to enhance contrast and visibility. The specified labels, relevant labels, and irrelevant labels are marked with dark green, light green, and red, respectively.**

**Table 18: The results of competitors and our method with the maximum iteration 100 and  $\delta = 2$  on COCO under different  $k$  values and sizes of randomly selected  $S$ , where  $\Delta$  refers to the difference between the original value and the perturbed value of corresponding metrics.  $\downarrow$  means the smaller the value the better, and  $\uparrow$  is the opposite. The best results under each set of parameters are bolded.**

$k$	$ S $	Methods	$\Delta T_k \text{Acc} \downarrow$	$\Delta P@k \downarrow$	$\Delta mAP@k \downarrow$	$\Delta NDCG@k \downarrow$	$\Delta I \uparrow$	APer $\downarrow$
3	2	ML-CW-U	0.6470	0.4900	0.6068	0.5478	1.8650	1.4768
		$k$ Fool	0.6190	0.3860	0.4428	0.3733	1.5900	10.9493
		$T_k$ ML-AP-U	0.6470	0.4810	0.6062	0.5443	1.9280	1.2629
		$T_k$ MIA(Ours)	<b>0.3700</b>	<b>0.2250</b>	<b>0.2652</b>	<b>0.2213</b>	<b>1.9970</b>	<b>1.0867</b>
	3	ML-CW-U	0.7300	0.3417	0.4647	0.3715	1.9050	1.4998
		$k$ Fool	0.6470	0.2746	0.3104	0.3104	1.9270	6.9378
		$T_k$ ML-AP-U	0.7330	0.3400	0.4703	0.3762	1.9780	1.2742
		$T_k$ MIA(Ours)	<b>0.5060</b>	<b>0.2166</b>	<b>0.2755</b>	<b>0.2114</b>	<b>2.0540</b>	<b>1.2499</b>
5	2	ML-CW-U	0.4620	0.4660	0.6133	0.5554	1.7510	1.8564
		$k$ Fool	0.4520	0.3630	0.4465	0.3655	1.5520	22.5433
		$T_k$ ML-AP-U	0.4610	0.4678	0.6231	0.5641	1.8540	1.6072
		$T_k$ MIA(Ours)	<b>0.2830</b>	<b>0.1828</b>	<b>0.2265</b>	<b>0.1739</b>	<b>1.9830</b>	<b>1.2318</b>
	3	ML-CW-U	0.5420	0.3104	0.4624	0.3788	1.8570	1.7330
		$k$ Fool	0.4980	0.2558	0.3229	0.2420	1.8240	13.9070
		$T_k$ ML-AP-U	0.5530	0.3086	0.4722	0.3868	1.9200	1.4759
		$T_k$ MIA(Ours)	<b>0.3480</b>	<b>0.1690</b>	<b>0.2301</b>	<b>0.1699</b>	<b>2.0550</b>	<b>1.2978</b>
	5	ML-CW-U	0.6311	0.1621	0.2189	0.1527	1.9417	1.4682
		$k$ Fool	0.5194	0.1271	0.1531	0.0986	<b>2.0291</b>	5.9820
		$T_k$ ML-AP-U	0.5776	0.1446	0.1994	0.1386	1.9514	1.2364
		$T_k$ MIA(Ours)	<b>0.4660</b>	<b>0.1097</b>	<b>0.1328</b>	<b>0.0870</b>	2.0048	<b>1.1073</b>
10	2	ML-CW-U	0.1111	0.4270	0.5957	0.5494	1.6984	2.1748
		$k$ Fool	0.1111	0.3158	0.4231	0.3408	1.3174	63.3469
		$T_k$ ML-AP-U	0.4063	0.4063	0.5802	0.5359	1.7142	1.8900
		$T_k$ MIA(Ours)	<b>0.0793</b>	<b>0.1698</b>	<b>0.2141</b>	<b>0.1501</b>	<b>1.9682</b>	<b>1.2652</b>
	3	ML-CW-U	0.1905	0.3286	0.4994	0.4258	1.9524	2.0335
		$k$ Fool	0.1904	0.2428	0.3426	0.2379	1.8095	41.4890
		$T_k$ ML-AP-U	0.1904	0.2761	0.4655	0.3921	1.8571	1.6844
		$T_k$ MIA(Ours)	<b>0.1904</b>	<b>0.1857</b>	<b>0.2730</b>	<b>0.1908</b>	<b>2.0476</b>	<b>1.5473</b>
	5	ML-CW-U	1.0000	0.2000	0.2056	0.1315	2.0000	2.4546
		$k$ Fool	1.0000	0.1499	0.1661	0.1012	2.0000	15.6337
		$T_k$ ML-AP-U	1.0000	0.1499	0.2414	0.1737	2.0000	2.2539
		$T_k$ MIA(Ours)	<b>1.0000</b>	<b>0.0999</b>	<b>0.1289</b>	<b>0.0723</b>	<b>2.0000</b>	<b>1.8203</b>

**Table 19: The rest results of competitors and our method with the maximum iteration 300 and  $\delta = 2$  on COCO under different  $k$  values and sizes of randomly selected  $S$ , where  $\Delta$  refers to the difference between the original value and the perturbed value of corresponding metrics.  $\downarrow$  means the smaller the value the better, and  $\uparrow$  is the opposite. The best results under each set of parameters are bolded.**

$k$	$ S $	Methods	$\Delta T_k \text{Acc} \downarrow$	$\Delta P@k \downarrow$	$\Delta mAP@k \downarrow$	$\Delta NDCG@k \downarrow$	$\Delta I \uparrow$	APer $\downarrow$
3	2	ML-CW-U	0.6850	0.5367	0.6568	0.5965	2.0000	1.6477
		$k$ Fool	0.6260	0.3943	0.4527	0.3833	1.6360	18.2784
		$T_k$ ML-AP-U	0.6640	0.4933	0.6239	0.5599	2.0000	1.3426
		$T_k$ MIA(Ours)	<b>0.3740</b>	<b>0.2240</b>	<b>0.2642</b>	<b>0.2203</b>	<b>2.0000</b>	<b>1.0935</b>
	3	ML-CW-U	0.7820	0.3693	0.5004	0.4012	2.0250	1.6598
		$k$ Fool	0.6580	0.2813	0.3183	0.2376	1.9470	10.0718
		$T_k$ ML-AP-U	0.7540	0.3533	0.4887	0.3919	2.0260	1.3381
		$T_k$ MIA(Ours)	<b>0.4860</b>	<b>0.2087</b>	<b>0.2684</b>	<b>0.2063</b>	<b>2.0460</b>	<b>1.2561</b>
10	2	ML-CW-U	0.1111	0.4635	0.6450	0.5938	2.0000	2.3947
		$k$ Fool	0.1111	0.2952	0.4132	0.3331	1.3333	61.5793
		$T_k$ ML-AP-U	<b>0.1111</b>	0.4555	0.6351	0.5859	2.0000	2.0634
		$T_k$ MIA(Ours)	0.3450	<b>0.1704</b>	<b>0.2319</b>	<b>0.1716</b>	<b>2.0710</b>	<b>1.3283</b>
	3	ML-CW-U	0.1905	0.3381	0.5166	0.4420	2.0000	2.1017
		$k$ Fool	<b>0.1904</b>	0.2476	0.3374	0.2406	1.8095	38.4887
		$T_k$ ML-AP-U	0.1904	0.3095	0.4889	0.4174	2.0000	1.8292
		$T_k$ MIA(Ours)	0.4514	<b>0.1087</b>	<b>0.1308</b>	<b>0.0862</b>	<b>2.0145</b>	<b>1.1295</b>
	5	ML-CW-U	<b>0.5000</b>	0.1000	<b>0.1163</b>	<b>0.0698</b>	2.0000	<b>1.6352</b>
		$k$ Fool	0.5000	0.0999	0.1211	0.0714	2.0000	17.5303
		$T_k$ ML-AP-U	0.5000	0.0999	0.1914	0.1418	2.0000	2.2226
		$T_k$ MIA(Ours)	1.0000	<b>0.0999</b>	0.1472	0.0805	<b>2.0000</b>	1.6473

**Table 20: The results of competitors and our method with the maximum iteration 500 and  $\delta = 3$  on COCO under different  $k$  values and sizes of randomly selected  $S$ , where  $\Delta$  refers to the difference between the original value and the perturbed value of corresponding metrics.  $\downarrow$  means the smaller the value the better, and  $\uparrow$  is the opposite. The best results under each set of parameters are bolded.**

$k$	$ S $	Methods	$\Delta T_k \text{Acc} \downarrow$	$\Delta P@k \downarrow$	$\Delta mAP@k \downarrow$	$\Delta NDCG@k \downarrow$	$\Delta I \uparrow$	APer $\downarrow$
3	3	ML-CW-U	0.9740	0.7177	0.8457	0.7674	3.0000	2.0312
		$k$ Fool	0.8300	0.4526	0.5194	0.4236	2.2590	32.7336
		$T_k$ ML-AP-U	0.9630	0.6996	0.8305	0.7513	3.0000	1.6714
		$T_k$ MIA(Ours)	<b>0.5890</b>	<b>0.3166</b>	<b>0.3773</b>	<b>0.3108</b>	<b>3.0000</b>	<b>1.5890</b>
5	3	ML-CW-U	0.6390	0.6286	0.7825	0.7180	3.0000	2.2634
		$k$ Fool	0.5690	0.4020	0.5021	0.4124	2.1600	100.0775
		$T_k$ ML-AP-U	0.6370	0.6128	0.7758	0.7078	3.0000	1.8995
		$T_k$ MIA(Ours)	<b>0.4280</b>	<b>0.2480</b>	<b>0.3110</b>	<b>0.2395</b>	<b>3.0000</b>	<b>1.5833</b>
	5	ML-CW-U	0.9272	0.3592	0.5382	0.4132	3.0243	2.0656
		$k$ Fool	0.7087	0.2359	0.2947	<b>0.2044</b>	2.7475	35.2941
		$T_k$ ML-AP-U	0.9077	0.3262	0.5086	0.3872	3.0145	1.7110
		$T_k$ MIA(Ours)	<b>0.6553</b>	<b>0.2106</b>	<b>0.2909</b>	0.2053	<b>3.0388</b>	<b>1.6672</b>
10	3	ML-CW-U	0.1905	0.5905	0.7404	0.6973	3.0000	2.4183
		$k$ Fool	0.1904	0.3476	0.4753	0.3706	1.8571	101.8643
		$T_k$ ML-AP-U	0.1904	0.5571	0.7413	0.6858	3.0000	2.1472
		$T_k$ MIA(Ours)	<b>0.1904</b>	<b>0.2380</b>	<b>0.3179</b>	<b>0.2297</b>	<b>3.0000</b>	<b>1.7015</b>
	5	ML-CW-U	1.0000	0.4000	0.6626	0.5137	3.0000	2.9090
		$k$ Fool	1.0000	<b>0.2500</b>	<b>0.2865</b>	<b>0.1769</b>	2.0000	10.2294
		$T_k$ ML-AP-U	1.0000	0.3999	0.5386	0.4225	3.0000	2.5256
		$T_k$ MIA(Ours)	<b>1.0000</b>	0.3000	0.4126	0.2507	<b>3.0000</b>	<b>2.3050</b>

**Table 21: The results of competitors and our method with the maximum iteration 100 and  $\delta = 2$  on NUS under different  $k$  values and sizes of randomly selected  $\mathcal{S}$ , where  $\Delta$  refers to the difference between the original value and the perturbed value of corresponding metrics.  $\downarrow$  means the smaller the value the better, and  $\uparrow$  is the opposite. The best results under each set of parameters are bolded.**

$k$	$ \mathcal{S} $	Methods	$\Delta T_k \text{Acc} \downarrow$	$\Delta P@k \downarrow$	$\Delta mAP@k \downarrow$	$\Delta NDCG@k \downarrow$	$\Delta I \uparrow$	APer $\downarrow$
2	2	ML-CW-U	0.4690	0.3240	0.3710	0.3337	1.2820	1.3689
		$k$ Fool	0.7420	0.5160	0.5595	0.5042	<b>1.8820</b>	19.0300
		$T_k$ ML-AP-U	0.5270	0.3670	0.4235	0.3819	1.3780	<b>1.1840</b>
		$T_k$ MIA(Ours)	<b>0.3740</b>	<b>0.2325</b>	<b>0.2600</b>	<b>0.2253</b>	1.5990	1.2962
3	2	ML-CW-U	0.2980	0.1963	0.2546	0.2240	0.9200	1.5029
		$k$ Fool	0.6710	0.5436	0.5909	0.5443	<b>1.9110</b>	44.2922
		$T_k$ ML-AP-U	0.3570	0.2466	0.3167	0.2811	1.0300	<b>1.3011</b>
		$T_k$ MIA(Ours)	<b>0.2560</b>	<b>0.1536</b>	<b>0.1775</b>	<b>0.1473</b>	1.3580	1.3524
	3	ML-CW-U	<b>0.3420</b>	<b>0.1433</b>	0.1851	0.1436	1.0320	1.4344
		$k$ Fool	0.6340	0.2740	0.3226	0.2462	<b>2.0050</b>	12.0781
		$T_k$ ML-AP-U	0.4050	0.1743	0.2347	0.1844	1.1380	<b>1.2434</b>
		$T_k$ MIA(Ours)	0.3770	0.1486	<b>0.1730</b>	<b>0.1280</b>	1.3880	1.3605
5	2	ML-CW-U	0.2670	0.1332	0.1819	0.1477	0.4920	1.6755
		$k$ Fool	0.6020	0.5782	0.6469	0.5876	<b>1.8700</b>	85.8662
		$T_k$ ML-AP-U	0.2820	0.1678	0.2263	0.1918	0.6020	1.4976
		$T_k$ MIA(Ours)	<b>0.2480</b>	<b>0.1196</b>	<b>0.1397</b>	<b>0.1008</b>	1.0620	<b>1.4137</b>
	3	ML-CW-U	0.2522	0.1009	0.1334	0.1022	0.6959	1.6779
		$k$ Fool	0.6171	0.3506	0.4237	0.3335	<b>2.0125</b>	35.2714
		$T_k$ ML-AP-U	0.2593	0.1202	0.1674	0.1330	0.7781	<b>1.4853</b>
		$T_k$ MIA(Ours)	<b>0.2432</b>	<b>0.0994</b>	<b>0.1194</b>	<b>0.0846</b>	1.0930	1.5154
	5	ML-CW-U	0.3750	0.0833	0.1124	0.0716	1.2083	1.2708
		$k$ Fool	0.5416	0.1333	0.1572	0.1048	<b>2.1666</b>	3.2104
		$T_k$ ML-AP-U	<b>0.2916</b>	<b>0.0750</b>	0.1001	0.0693	1.3750	1.1406
		$T_k$ MIA(Ours)	0.3333	0.0833	<b>0.0936</b>	<b>0.0609</b>	1.5416	<b>1.0140</b>

**Table 22: The rest results of competitors and our method with the maximum iteration 300 and  $\delta = 2$  on NUS under different  $k$  values and sizes of randomly selected  $\mathcal{S}$ , where  $\Delta$  refers to the difference between the original value and the perturbed value of corresponding metrics.  $\downarrow$  means the smaller the value the better, and  $\uparrow$  is the opposite. The best results under each set of parameters are bolded.**

$k$	$ \mathcal{S} $	Methods	$\Delta T_k \text{Acc} \downarrow$	$\Delta P@k \downarrow$	$\Delta mAP@k \downarrow$	$\Delta NDCG@k \downarrow$	$\Delta I \uparrow$	APer $\downarrow$
2	2	ML-CW-U	0.7630	0.5495	0.6230	0.5677	1.8840	2.0010
		$k$ Fool	0.7530	0.5285	0.5737	0.5186	1.9030	28.4019
		$T_k$ ML-AP-U	0.7930	0.5720	0.6550	0.5971	<b>1.9250</b>	<b>1.6244</b>
		$T_k$ MIA(Ours)	<b>0.5220</b>	<b>0.3475</b>	<b>0.3837</b>	<b>0.3408</b>	1.9170	1.6469
3	2	ML-CW-U	0.6190	0.4503	0.5606	0.5017	1.7210	2.2771
		$k$ Fool	0.6680	0.5396	0.5857	0.5385	<b>1.9140</b>	49.0967
		$T_k$ ML-AP-U	0.6640	0.5053	0.6261	0.5637	1.8390	1.8981
		$T_k$ MIA(Ours)	<b>0.4110</b>	<b>0.2673</b>	<b>0.3030</b>	<b>0.2577</b>	1.8160	<b>1.8075</b>
	3	ML-CW-U	0.7090	0.3383	0.4390	0.3504	1.7770	2.2154
		$k$ Fool	0.6360	0.2733	0.3235	0.2467	<b>2.0040</b>	13.1977
		$T_k$ ML-AP-U	0.7770	0.3790	0.5008	0.4029	1.8780	<b>1.8377</b>
		$T_k$ MIA(Ours)	<b>0.6010</b>	<b>0.2730</b>	<b>0.3158</b>	<b>0.2412</b>	1.8880	1.9296

**Table 23: The results of competitors and our method with the maximum iteration 500 and  $\delta = 3$  on NUS under different  $k$  values and sizes of randomly selected  $S$ , where  $\Delta$  refers to the difference between the original value and the perturbed value of corresponding metrics.  $\downarrow$  means the smaller the value the better, and  $\uparrow$  is the opposite. The best results under each set of parameters are bolded.**

$k$	$ S $	Methods	$\Delta T_k \text{Acc} \downarrow$	$\Delta P@k \downarrow$	$\Delta mAP@k \downarrow$	$\Delta NDCG@k \downarrow$	$\Delta I \uparrow$	$APer \downarrow$
3	3	ML-CW-U	0.9340	0.6833	0.8049	0.7308	2.8030	2.8624
		$kFool$	0.9630	0.7353	0.8002	0.7337	2.8630	83.3383
		$T_k ML-AP-U$	0.9680	0.7450	0.8606	0.7917	<b>2.9390</b>	<b>2.3481</b>
		$T_k MIA(Ours)$	<b>0.7680</b>	<b>0.4893</b>	<b>0.5452</b>	<b>0.4729</b>	2.8600	2.5979
5	3	ML-CW-U	0.6565	0.5574	0.7041	0.6318	2.5671	3.2198
		$kFool$	0.6905	0.6991	0.7644	0.7095	2.8246	162.6897
		$T_k ML-AP-U$	0.6762	0.6314	0.7772	0.7104	<b>2.8389</b>	<b>2.6935</b>
		$T_k MIA(Ours)$	<b>0.5402</b>	<b>0.3667</b>	<b>0.4086</b>	<b>0.3237</b>	2.6583	2.7339
	5	ML-CW-U	0.8750	0.3417	0.4689	0.3557	2.5833	2.9803
		$kFool$	<b>0.7500</b>	0.2666	0.3309	0.2337	<b>3.0000</b>	15.4970
		$T_k ML-AP-U$	0.9166	0.3666	0.5490	0.4223	2.9166	<b>2.4811</b>
		$T_k MIA(Ours)$	0.7916	<b>0.2749</b>	<b>0.3258</b>	<b>0.2214</b>	2.9580	2.5540